Concept-Driven Continual Learning

Anonymous authors
Paper under double-blind review

Abstract

This paper introduces novel solutions to the challenge of catastrophic forgetting in continual learning: **Interpretability Guided Continual Learning** (IG-CL) and **Intrinsically Interpretable Neural Network** (IN2). These frameworks bring interpretability into continual learning, systematically managing human-understandable concepts within neural network models to enhance knowledge retention from previous tasks. Our methods are designed to enhance interpretability, providing transparency and control over the continual training process. While our primary focus is to provide a new framework to design continual learning algorithms based on interpretability instead of improving performance, we observe that our methods often surpass existing ones: IG-CL employs interpretability tools to guide neural networks, showing an improvement of up to 1.4% in average incremental accuracy over existing methods; IN2, inspired by the Concept Bottleneck Model, adeptly adjusts concept units for both new and existing tasks, reducing average incremental forgetting by up to 9.1%. Both frameworks demonstrate superior performance compared to exemplar-free methods and are competitive with exemplar-based methods. When combined with exemplar-based strategies, they further improve the performance by up to 18%. These advancements represent a significant step in addressing the limitations of current continual learning methods, offering efficient and interpretable approaches that do not require additional memory for past data.

1 Introduction

Continual learning is a crucial aspect of machine learning, empowering models to adapt and improve as they encounter new data over time. This dynamic learning process, however, faces a significant hurdle known as "catastrophic forgetting." This phenomenon, where a model forgets previously learned information upon acquiring new knowledge, is largely attributed to the shift in input distribution with changing tasks. According to van de Ven et al. (2022); De Lange et al. (2021), there are three primary settings in continual learning: class incremental, task incremental, and domain incremental. Our focus in this paper is on the class incremental setting, identified as the most challenging setting among three due to its pronounced susceptibility to catastrophic forgetting, as detailed in van de Ven et al. (2022); Chaudhry et al. (2018a); De Lange et al. (2021).

Current strategies in continual learning fall into the following main categories: **Exemplar-free** and **Exemplar-based** methods. **Exemplar-free** methods do not rely on data from old tasks, like *regularization-based* methods that introduce constraints to preserve old knowledge; *architecture-based* methods that adapt the model's structure for new tasks. On the other hand, **Exemplar-based** methods, also known as *replay-based* methods, involve revisiting previous data. *Replay-based* methods generally outperform others but require extra memory for data storage. Despite existing methods show some promise, they still lack in performance and many of them still have serious catastrophic forgetting problems. This gap highlights the need for more systematic and understandable approaches in continual learning.

In parallel, there is a growing body of research dedicated to deciphering the role of neurons in neural networks. Pioneering studies, such as (Bau et al., 2017; 2020; Oikarinen & Weng, 2022; Hernandez et al., 2022), have highlighted "concept units" – neurons that closely align with concepts easily understood by humans. Our research reveals a critical gap in current continual learning algorithms: While previous continual learning algorithms generally fail to effectively preserve these concept units, our research reveals the advantage of

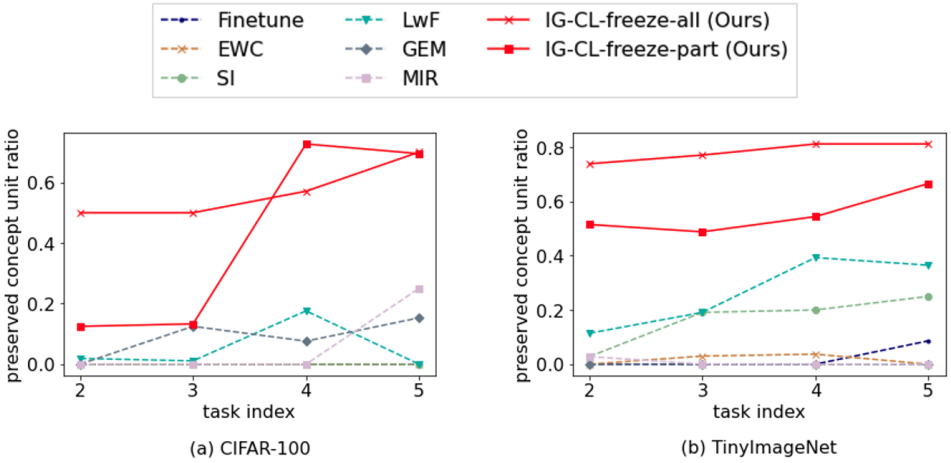

Figure 1: IG-CL's concept evolution in (a) CIFAR-100 and (b) TinyImageNet. Tasks' classes are in Appendix D.3. The results show that existing work perform poorly on preserving the learned concepts hence suffers from catastrophic forgetting problem, while the proposed IG-CL can preserve the concepts from previous classes. The values are in Table 5 of Appendix A.1.

leveraging interpretability for mitigating catastrophic forgetting. This key finding, detailed in Figure 1, has shaped our approach to developing new continual learning frameworks.

In this paper, we present two novel frameworks, **Interpretability Guided Continual Learning** (IG-CL) and **Intrinsically Interpretable Neural Network** (IN2), to address the issue of catastrophic forgetting in continual learning. Unlike existing approaches that lack interpretability, our methods stand out by incorporating interpretability, enabling systematic management of human-understandable concepts within the model, which enhances knowledge retention from prior tasks. Our contributions are the following:

- Our first method, IG-CL, uses interpretability tools (Bau et al., 2020; Oikarinen & Weng, 2022) to guide neural networks in continual learning. IG-CL has proven to be effective in our extensive experiments, outperforming existing methods by achieving up to 1.4% higher average incremental accuracy.

- Our second method, IN2, is a novel framework based on the Concept Bottleneck Model (CBM) (Koh et al., 2020), tailored for continual learning. IN2 is engineered to maintain and adapt concept units corresponding to both old and new tasks, further reducing average incremental forgetting by up to 9.1% compared to existing methods. Different from IG-CL, IN2 modifies the model's architecture and inherit interpretability from CBM.

- To our best knowledge, IG-CL and IN2 are the first general approach to make the learned knowledge and the training process transparent and interpretable in the continual learning setting.

Our primary aim is to leverage interpretability to provide transparency and control over retained knowledge and the training process, addressing gaps in the current literature. IG-CL and IN2 bridge interpretability and continual learning from two perspectives. IG-CL brings interpretability to continual learning by using external interpretability tools to guide models. On the other hand, IN2 tailor interpretable models like CBM for continual learning by leveraging their own interpretability. While our focus is on proposing a new framework to design continual learning algorithms based on interpretability, we observe that our methods often surpass existing ones. For instance, our approach outperforms exemplar-free methods in average incremental accuracy and is competitive with exemplar-based methods. When combined with exemplar-based strategies, our methods enhance their performance by up to 18%. Additionally, our methods are memory-efficient, requiring no extra memory space for storing data from previous tasks. The benefits of our methods are summarized in Table 1. Interpretability is key distinguishing feature of our approach compared to existing methods.

Table 1: Comparison of our method against existing methods for continual learning.

	(I) Scalability		(II) Flexibility	(III) Interpretability
Method:	Only need one backbone	Without memory buffers	For any architecture	
Exemplar-free				
EWC Kirkpatrick et al. (2017)	**Yes**	**Yes**	**Yes**	No
SI Zenke et al. (2017)	**Yes**	**Yes**	**Yes**	No
LwF Li & Hoiem (2017)	**Yes**	**Yes**	**Yes**	No
Adam-NSCL Wang et al. (2021)	**Yes**	**Yes**	**Yes**	No
SSRE Zhu et al. (2022)	**Yes**	**Yes**	**Yes**	No
DEN Yoon et al. (2017)	**Yes**	**Yes**	**Yes**	No
ICICLE Rymarczyk et al. (2023)	**Yes**	**Yes**	No	△ (part-based prototype)
Exemplar-based				
GEM Lopez-Paz & Ranzato (2017)	**Yes**	No	**Yes**	No
MIR Aljundi et al. (2019)	**Yes**	No	**Yes**	No
DER Yan et al. (2021)	No	No	No	No
IG-CL (Ours)	**Yes**	**Yes**	**Yes**	**Yes, text-based concept (more general)**
IN2 (Ours)	**Yes**	**Yes**	**Yes**	**Yes, text-based concept (more general)**

2 Background and Related Work

2.1 Continual Learning

To mitigate catastrophic forgetting in continual learning, several methods have been proposed. They can be categorized into **Exemplar-free** and **Exemplar-based** methods. For **Exemplar-free** methods, it consists of two streams: regularization-based methods and architecture-based method. The key idea of regularization-based methods is to add additional terms in the loss function to constrain model parameters to not change too much from previous tasks (Kirkpatrick et al., 2017; Zenke et al., 2017; Li & Hoiem, 2017; Jung et al., 2016; Dhar et al., 2019; Castro et al., 2018; Hu et al., 2019; Lee et al., 2019; Aljundi et al., 2018; Chaudhry et al., 2018a; Lee et al., 2017; Schwarz et al., 2018). On the other hand, architecture-based methods modify the model's architecture or parameters when learning new tasks, by dynamic expansion or pruning (Rusu et al., 2016; Yoon et al., 2017; Xu & Zhu, 2018; Yan et al., 2021; Li et al., 2019; Serra et al., 2018; Wang et al., 2021; Zhu et al., 2022). For **Exemplar-based** method, it is also known as replay-based methods, whose spirit is to store previous tasks' information and train the model with new tasks jointly (Lopez-Paz & Ranzato, 2017; Rebuffi et al., 2017; Chaudhry et al., 2018b; Rolnick et al., 2019; Hou et al., 2019; Wu et al., 2019; Buzzega et al., 2020; Wang et al., 2022; Guo et al., 2022; Liu et al., 2021; Aljundi et al., 2019). More details of these methods is in Appendix D.2.

Meanwhile, some works focus on the theoretical aspect of continual learning (Peng et al., 2023; Peng & Risteski, 2022; Cao et al., 2022; Ruvolo & Eaton, 2013; Pentina & Urner, 2016; Chen et al., 2022; Kim et al., 2022). However, none of these methods are able to control human-interpretable concepts directly, which makes them lack interpretability. Indeed, interpretability is one of the main differences between our methods and existing methods. Recent works (Marconato et al., 2023) (Rymarczyk et al., 2023) connects interpretability with continual learning. They focus on part-based prototype concepts or neuro-symbolic concepts. Our work focuses on text-based concepts instead, which allows more general interpretability. Meanwhile, they are only suitable for particular model architectures whereas our methods are suitable for any CNN-based models.

2.2 Neuron-Level Interpretation and Concept Bottleneck Models

Several works (Bau et al., 2017; 2020; Oikarinen & Weng, 2022; Hernandez et al., 2022; Mu & Andreas, 2020) provide automated descriptions of the roles of individual neurons in deep vision models, and do extensive studies for their methods' interpretability. Typically these methods generate a description by analyzing what kinds of inputs result in high activations for the given neuron. For example, Network Dissection (Bau et al., 2020) identifies the concepts of individual neurons by comparing the neuron's activation map to concept annotated data. A more recent work CLIP-Dissect (Oikarinen & Weng, 2022) eliminates the need of concept annotated data by leveraging the Contrastive Language-Image Pre-training (CLIP) model (Radford et al., 2021) and several similarity functions. Detailed introduction of CLIP-Dissect is in Appendix D.2.2. In this paper, we explore a departure from the typical emphasis on refining interpretability tools, instead utilizing

them to guide continual learning processes. Our work focuses on the computer vision domain since the interpretability tools in the domain have made significant progress. It can be applied to other domains like NLP with their interpretability tools like Sajjad et al. (2022) potentially in the future.

Concept Bottleneck Model (CBM) (Koh et al., 2020) has a layer called Concept Bottleneck Layer (CBL) where each neuron corresponds to a human interpretable concept. The idea of CBL is to create an meaningful concept mapping from black-box representations to a layer that contains a human-interpretable concept set C, allowing effective intervention and explaining the model predictions. The concept set C generation depends on each CBM. The original CBM (Koh et al., 2020) requires datasets to provide concept sets. Recent works (Oikarinen et al., 2023; Yuksekgonul et al., 2022) try to address it since concept annotations is expensive and hard to collect. Specifically, Label-Free CBM (LF-CBM) (Oikarinen et al., 2023) generates concepts from task information. Detailed introduction of LF-CBM is in Appendix D.2.2. The primary focus of these CBM works is only on single task and does not consider the challenging continual learning setting. In contrast, our IN2 is tailored for continual learning with a new learning procedure that enables it to learn a series of tasks, which generalizes CBM-based methods to continual learning.

3 Our first method: IG-CL

Overview. To address catastrophic forgetting, we aim to manage concepts learned by models in an interpretable manner. We introduce two frameworks: **Interpretability Guided Continual Learning** (IG-CL) in this section and **Intrinsically Interpretable Neural Network** (IN2) in the next section. IG-CL uses an interpretability tool to steer the learning process, identifying and preserving previously learned concepts to prevent forgetting. This approach enhances model comprehension and has shown to improve incremental accuracy by up to 1.4%. Building on this, IN2 incorporates interpretable neurons that are systematically integrated and controlled, further reducing forgetting by up to 9.1% in our experiments. Figure 2 illustrates the key steps in IG-CL, and the details of each step are described below. IG-CL's full algorithm is summarized in Algorithm 1 in Appendix C.2.

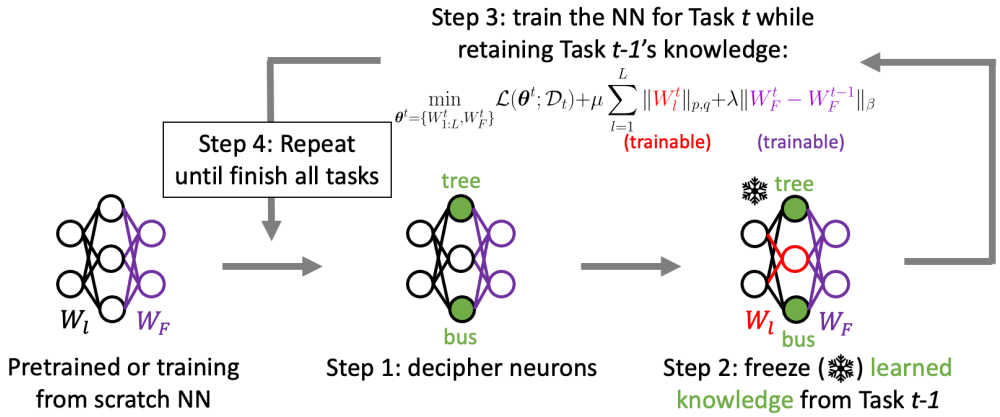

Figure 2: IG-CL's procedure.

3.1 Step 1: Decipher network

Initially, we use a neuron-interpretability tool to decipher the interpretable neurons in the model. Interpretable neurons are defined as those whose activations correspond closely to human-understandable concepts (e.g. "red", "stripes", "windy", etc). A model, denoted as θ, consists of a feature extractor $\{W_l\}_{l=1}^{L}$, also known as a backbone, and a prediction layer W_F. Our goal is to preserve the important concepts learned from the previous tasks. Previous work (Bau et al., 2020) analyzes the concept neurons in each layer, and finds out that high-level concept neurons emerge in the deep layers. Low-level concepts are basic descriptions like colors or scripts, while high-level concepts are objects or components of the images. The high-level concepts are specific to the classes in the previous tasks, which needed to be preserved. Therefore, we apply the

interpretability tool on the last layer of the feature extractor W_L to decipher the neurons. The discovered interpretable neurons are called **concept units**. Existing neuron interpretability tools (Bau et al., 2017; Oikarinen & Weng, 2022) are directly applicable to detect the concepts of neurons in our framework.

3.2 Step 2: Freezing the learned knowledge

Second, we want to freeze the concept units in the model to preserve the learned knowledge. These concept units emerged in the network during learning the current task $t-1$. To prevent catastrophic forgetting, it is desired to preserve these concept units when learning a new task t. To achieve this, we propose to find and freeze these task-related neurons when learning the new task t by finding a sub-network which links all related neurons. In practice, this can be implemented by using Breadth First Search (BFS) from the concept unit in W_L to the input layer W_1. Define two neurons are connected when the weight exceeds threshold τ. We propose two ways to freeze the subnetworks to preserve the learned knowledge by different degrees:

- **freeze-all** Freeze all weights connected to neurons in any concept units' subnetwork.
- **freeze-part** Only freeze input weights to all neurons in the subnetworks, leaving output weights trainable.

We describe Step 2 mathematically in Line 7 - Line 19 of Algorithm 1 in Appendix C.2.

The **freeze-part** method leaves the output weights of the neurons in the subnetwork trainable, which may have a better ability to learn new tasks. For **freeze-all** method, it isolates the subnetworks from the rest of the model which is expected to promote less forgetting. An illustration of these two methods is in Figure 3. The experiment results in Section 5 show that the **freeze-all** method forgets less, while the **freeze-part** method has better learnability for a longer series of tasks. This step is summarized in Algorithm 1 Line 8-19.

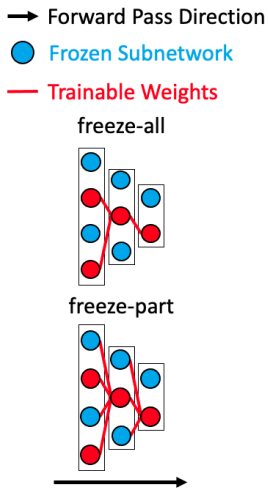

Figure 3: The illustration of two freezing subnetwork methods. Red nodes and lines stand for trainable unit and weights.

3.3 Step 3: Learning without forgetting

Next, we train the model on a new task t with Eq. (1). Let $\mathcal{D}_t$ be the data for task t. We have two goals when learning task t: regularize (1) the size of subnetworks and (2) W_F. To regularize the size of subnetworks described in Step 2, we choose $p=2, q=1$ and μ to regularize the number of activated units. Second, inspired by the regularization-based methods, we train the model with regularization $\beta=2$ on the W_F, which aims to prevent W_F from changing too much. But different from previous regularization-based methods, the preserved knowledge in our method is interpretable (as they are detected as interpretable concept units in Step 1, which can be easily understood through the text).

$$\min_{\boldsymbol{\theta}^t} \mathcal{L}(\boldsymbol{\theta}^t; \mathcal{D}_t) + \mu \sum_{l=1}^{L} \|W_l^t\|_{p,q} + \lambda \|W_F^t - W_F^{t-1}\|_\beta \tag{1}$$

Then, we will repeat Step 1 to 3 for task 2, 3 ... until the last task T, as illustrated in Figure 2.

3.4 Further Discussion

Interpretability. Unlike previous methods in continual learning, which lack interpretability due to their inability to clearly identify retained knowledge in a human-understandable manner, IG-CL simplifies the preservation process, ensuring clarity and straightforwardness. Notably, IG-CL is designed to be compatible with existing neuron interpretability tools (Bau et al., 2017; Oikarinen & Weng, 2022), allowing it to integrate seamlessly with multiple frameworks and enhance the transparency of the learning process. Nonetheless, the selection of interpretability tools affects IG-CL significantly. The generalizability of interpretability tools are the key to guide and improve continual learning. Therefore, it's essential that the interpretability tools we

selected to be flexible (e.g. open-vocabulary concepts). Meanwhile, they have to be efficient so the continual learning process will not be too long. Based on these criteria, in this work we use CLIP-Dissect (Oikarinen & Weng, 2022) as the tool to detect neuron concepts.

Ability to Share Concepts Among Tasks. IG-CL is designed to keep and reuse the learned concepts from old tasks. Experiment in Section 5.3, Appendix A.1 and B.6 study its ability and show that it outperforms baselines by up to 9% in forward transfer metric.

Efficiency. IG-CL framework is light since it does not need extra memory storage to store previous tasks' samples. Previous tasks' knowledge is stored within the model. Experiment on GPU usage in Appendix C.1 shows the efficiency of IG-CL.

4 Our second method: IN2

In Section 3, we introduced IG-CL as a novel interpretable method to identify and manage concept units in models for reducing catastrophic forgetting, marking it as a pioneering approach in the regularization-based category. Building on this, we now present the **Intrinsically Interpretable Neural Network** (IN2), a new architecture-based method that transforms any neural network into an interpretable framework designed for continual learning. IN2 uniquely maintains previously learned concept units while integrating new ones for upcoming tasks, demonstrating a reduction in average incremental forgetting by up to 9.1% over existing methods according to our experiments. Compared with IG-CL, IN2 does not need external interpretability tools since CBM provides interpretability. Figure 4 illustrates the procedure of IN2.

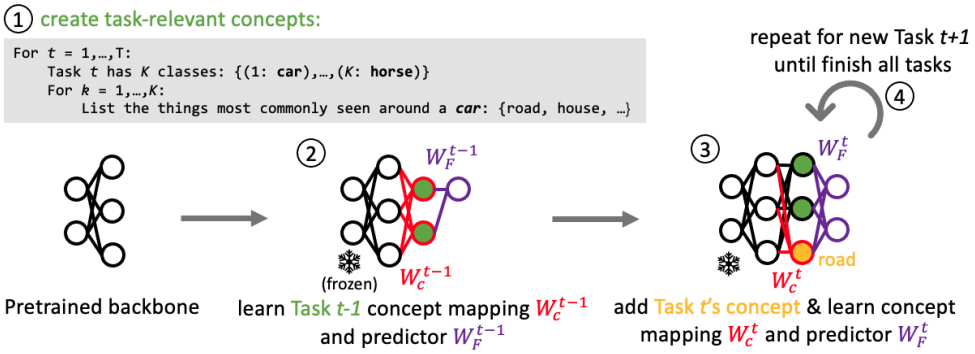

Figure 4: IN2's procedure.

4.1 Step 0: Set up CBM

For the first task, the learning procedure is the same as training a Concept Bottleneck Model (CBM) (Koh et al., 2020) on the first single task. In the continual learning setting, after learning the task $t-1$, the CBM has a concept set $\mathcal{C}^{t-1}$ and the concept mapping W_c^{t-1} in between the backbone and the prediction layer. We consider the setting that backbone $f(x)$ is frozen for reduced training cost, but our method also allows backbone being trained from scratch or finetuned. For task t, we create a task-relevant concept set c_k^t from its class labels k. Creation of the task-relevant concept sets depends on the Concept Bottleneck Model (CBM). For LF-CBM (Oikarinen et al., 2023), concept sets are generated by asking GPT-3 about the concepts related to the classes. For CBM (Koh et al., 2020), concept sets are predefined and provided in the dataset. In the following paragraphs of IN2's learning procedure, we consider the case that the model has learned $t-1$ tasks, and it is going to learn a new task t.

4.2 Step 1: Concept set expansion

In this step, we expand the concept set based on classes in new task t. Given the concept set from $t-1$ tasks as $\mathcal{C}^{t-1}$, we form a new concept set $\mathcal{C}^t$ by adding all concepts in c_k^t into $\mathcal{C}^{t-1}$. If certain concepts in c_k^t are already

present in $\mathcal{C}^{t-1}$, we include them nonetheless. This is because identical textual concepts across different tasks may exhibit distinct attributes, such as variations in color and shape. For example, concept "ship" might refer to "vessel" or "cargo ship" in different tasks. After the expansion, there are $|C^t| = |C^{t-1}| + |c_k^t|$ concepts in $\mathcal{C}^t$. The analysis of duplicate concepts and numbers are in Appendix C.3

4.3 Step 2: Learning the concept mapping

To preserve learned concepts, we keep the weights of the existing concepts from the concept mapping of the previous task. Given a new concept mapping for learning the task t is $W_c^t \in \mathbb{R}^{|C^t| \times d}$, we first inherit the concept mapping's weights from the previous model:

$$W_c^t[i,:] = W_c^{t-1}[i-1,:] \quad \forall i \in \{1, 2, ..., |C^{t-1}|\} \tag{2}$$

where $W_c^t[i,:]$ means the i-th row of the W_c^t. The second step is to learn W_c^t using the procedure of CBM. Take LF-CBM Oikarinen et al. (2023) as an example. LF-CBM aims to align the concept mapping with CLIP's (Radford et al., 2021) representation of the concepts. Therefore, the procedure is to maximize the similarity between concept mapping's $f_c^t(x) = W_c^t f(x)$ and CLIP's activation matrix. The second step can be done in two ways:

1. **Finetune**: We learn W_c^t on task t without additional constraints. We only initialize W_c^t with old concepts but these concepts will be changed on the new task.

2. **IN2**: We freeze the previous concepts' corresponding mapping in W_c^t to prevent them from changing. This strategy enables us to learn the mapping of new concepts without affecting the previously learned ones. This strategy makes IN2 light and interpretable. It eliminates the need for additional memory storage for previous tasks' samples, and provides transparency regarding the retained knowledge.

4.4 Step 3: Learning the prediction layer

Finally, we aim to learn the prediction layer without forgetting. First, we inherit prediction weights in W_F^{t-1} to W_F^t before the learning process. The idea is similar to Step 2, where $|C^{t-1}|$ concept output weights in W_F^t inherit the same weights from W_F^{t-1}. Again, the **Finetune** strategy is to learn W_F^t without any constraints. On the other hand, the **IN2** strategy follows the similar idea as IG-CL's Step 3 to learn the prediction layer with regularization γ and $\beta = 2$. Meanwhile, we control the sparsity of W_F by setting $\alpha = 1$ and λ. Given the dataset $\mathcal{D}_t = (\mathcal{X}^t, \mathcal{Y}^t)$, the training goal is to minimize the loss in Eq. (3) where $\mathcal{L}$ could be cross-entropy loss.

$$\mathcal{L}(W_F^t; f_c^t(\mathcal{X}^t), \mathcal{Y}^t) + \lambda \|W_F^t\|_\alpha + \gamma \|W_F^t - W_F^{t-1}\|_\beta \tag{3}$$

4.5 Further Discussion

Interpretability. IN2 is a versatile framework that supports various approaches for constructing CBMs (Koh et al., 2020; Yuksekgonul et al., 2022; Oikarinen et al., 2023), enhancing interpretability by allowing analysis of predictions in human-understandable terms, as illustrated in Figure 5. This interpretability also makes the progression of knowledge acquisition in continual learning transparent, a significant improvement over previous architecture-based methods, which lack clarity and interpretability on the knowledge integrated into the extended architecture. Similar to IG-CL, generalizability, efficiency and accuracy are the selection criteria for CBMs. Because the CBMs for IN2 have to be accurately applied on different data streams, and be efficient for smooth continual learning processes.

Ability to Share Concepts Among Tasks. IN2 is designed to keep the learned concepts from old tasks. Experiment in Section 5.3, Appendix A.2 and B.6 study IN2's ability, and show that it can improve GEM (Lopez-Paz & Ranzato, 2017) by up to 7.8% in forward transfer metric when combining with GEM.

5 Experiments

In Section 5.1, we introduce the datasets, evaluation metrics, baselines and other details in the experiment. In Section 5.2, we compare our methods with existing methods in standard metrics. In Section 5.3, we unveil the learned knowledge and the training process by leveraging IG-CL and IN2 interpretability. In Section 5.4, we conduct ablation studies for our methods to analyze the contributions to their superior performance. Due to page limit, additional experiments and discussions are in Appendix A, B and C. An overview of additional experiments is provided in the first page of Appendix as Appendix Outline.

5.1 Experiment setup

Dataset. To evaluate our methods, we perform experiments on two datasets: CIFAR-100 (Krizhevsky et al., 2009) and TinyImageNet (Le & Yang, 2015). Experiments on CIFAR-10 (Krizhevsky et al., 2009) and CUB-200 (Wah et al., 2011) are discussed in Appendix B and C. We consider $T = 5, 10, 20$ tasks scenario in class incremental setting. We use ResNet18 (He et al., 2016) as the experiment model. Experiment, dataset, result report and hyperparameter selection details are in Appendix D.1.

Evaluation Metrics. Following (Mirzadeh et al., 2022b; Chaudhry et al., 2018a), we use the standard evaluation metrics to evaluate our methods. Define $a_{i,j}$ as model's accuracy on j-th task after learning i-th task, $i \geq j$. When testing the performance on t-th task, the metrics' definitions are as follows:

- **Average Accuracy**: Measures the average model performance $A_t = \frac{1}{t}\sum_{i=1}^{t} a_{t,i}$
- **Average Forgetting**: Measures model performance drop on previous tasks $F_t = \frac{1}{t-1}\sum_{i=1}^{t-1} \max_{j\in(1,\dots,t-1)}(a_{j,i} - a_{t,i})$

However, these standard metrics only reflect models' performance at the final stage. Following recent works (Zhu et al., 2022; Carta et al., 2023; Zhou et al., 2023; Caccia et al., 2020; 2021; Koh et al., 2021), we also evaluate models throughout the stream. Specifically, we also report:

- **Average Incremental Accuracy**: $\bar{A}_T = \frac{1}{T-1}\sum_{t=2}^{T} A_t$
- **Average Incremental Forgetting**: $\bar{F}_T = \frac{1}{T-1}\sum_{t=2}^{T} F_t$

Baselines. We perform experiments on the following continual learning baselines:

- Finetune: the standard method where models are updated continuously on a series of tasks
- Exemplar-free methods
  - (regularization-based) EWC (Kirkpatrick et al., 2017), SI (Zenke et al., 2017), LwF (Li & Hoiem, 2017)
  - (architecture-based) Adam-NSCL (Wang et al., 2021), DEN (Yoon et al., 2017) in Appendix B.5.2, SSRE (Zhu et al., 2022) in Appendix B.5.1, ICICLE (Rymarczyk et al., 2023) in Appendix B.5.3
- Exemplar-based methods
  - GEM (Lopez-Paz & Ranzato, 2017) and MIR (Aljundi et al., 2019)

Notations and Details. For IG-CL, "IG-CL-freeze-x" means IG-CL with implementation freeze-all/ freeze-part in Step 2. For CBM based methods, "Finetune-CBM" means using **Finetune** strategy in Step 2 and Step 3, while "IN2" means using **IN2** strategy instead. "IN2-remove" means removing duplicate concepts in concept set expansion 4.2. "-GEM" and "-MIR" means combining our methods with GEM and MIR respectively. For baseline strategies, we use the implementations from a continual learning library Avalanche (Lomonaco et al., 2021). We also use Avalanche to implement our methods.

Here we discuss $T = 5$ experiment results in $\{\bar{A}_T, \bar{F}_T\}$. For different metrics $\{A_T, F_T\}$, please see Appendix B.3; for experiment results of $\{T = 10, 20\}$, please see Appendix B.4. The comparisons with SSRE (Zhu et al., 2022), DEN (Yoon et al., 2017) and ICICLE (Rymarczyk et al., 2023) are in Appendix B.5. We were not able to compare with DER (Yan et al., 2021) as their official code is incomplete. Due to scalability and efficiency, we use CLIP-Dissect (Oikarinen & Weng, 2022) as the interpretability tool for IG-CL, and LF-CBM (Oikarinen et al., 2023) for CBMs in IN2. Memory usage experiment is in Appendix C.1.

5.2 Quantitative Results

5.2.1 Comparison results for IG-CL

For IG-CL, the accuracy comparisons with existing works are in Table 2. Compared with the Exemplar-free methods, our method outperforms existing works by up to 1.4% in $\bar{A}_T$ and up to 1.3% in $\bar{F}_T$. Most of the time IG-CL performs better using freeze-all than with freeze-part. Meanwhile, the performance is comparable to or even better than Exemplar-based methods in some benchmarks. When combining IG-CL with Exemplar-based methods, both freeze-all and freeze-part tend to improve Exemplar-based method to achieve higher $\bar{A}_T$ by up to 5.1% and lower $\bar{F}_T$ by up to 18.0%. The experiment results show that IG-CL can make models more effective and forget less, either standalone or combining with other methods. Considering the experiment results of 10-task and 20-task scenario in Appendix B.4, we observe that freeze-part has better performance when task number is bigger. Overall, the freeze-all approach is suitable for a limited number of tasks and emphasizes preserving learned knowledge, while the freeze-part approach is more appropriate for scenarios involving a large number of tasks.

Table 2: Accuracy comparison for IG-CL. ↑ means larger values are better, while ↓ means smaller values are better. Underline means the strongest baseline, and **boldface** means the best number. In the **Ours Improvement** rows, +/- measures our best number minus the strongest baseline, and the value is in blue if our improvement is statistically significant. Our methods outperform the baselines on both $\bar{A}_T$ and $\bar{F}_T$.

	CIFAR-100, 5T		TinyImagenet, 5T	
	$\bar{A}_T \uparrow$	$\bar{F}_T \downarrow$	$\bar{A}_T \uparrow$	$\bar{F}_T \downarrow$
Exemplar-free baselines				
Finetune	20.47 ± 0.67	63.02 ± 0.45	16.82 ± 2.18	49.80 ± 0.57
EWC	20.97 ± 0.55	62.56 ± 0.29	16.19 ± 2.65	48.42 ± 0.39
SI	17.75 ± 1.37	59.31 ± 1.93	13.07 ± 2.57	44.71 ± 2.28
LwF	12.74 ± 2.15	63.66 ± 2.40	16.09 ± 3.25	49.43 ± 1.26
Adam-NSCL	17.45 ± 2.35	59.54 ± 3.04	17.90 ± 2.57	44.98 ± 0.74
Ours				
IG-CL-freeze-all	**22.37 ± 1.20**	**58.75 ± 0.26**	**18.19 ± 0.76**	**43.39 ± 0.92**
IG-CL-freeze-part	21.73 ± 0.79	60.51 ± 0.35	18.08 ± 0.56	46.00 ± 0.66
Ours Improvement	**+1.40**	+0.56	+1.37	+1.32
Exemplar-based baselines				
GEM	23.02 ± 1.65	60.63 ± 4.12	11.29 ± 2.62	41.30 ± 1.67
Ours				
IG-CL-freeze-all-GEM	**28.18 ± 2.36**	**42.61 ± 2.12**	**12.49 ± 1.87**	**37.78 ± 1.04**
IG-CL-freeze-part-GEM	25.62 ± 2.08	52.39 ± 3.24	12.06 ± 1.58	42.67 ± 2.79
Ours Improvement	**+5.16**	**+18.02**	+1.20	**+3.52**
Exemplar-based baselines				
MIR	27.26 ± 0.93	53.02 ± 2.84	17.81 ± 0.82	44.60 ± 2.43
Ours				
IG-CL-freeze-all-MIR	27.04 ± 1.08	**51.66 ± 3.11**	19.95 ± 2.41	**43.08 ± 0.95**
IG-CL-freeze-part-MIR	**27.59 ± 0.62**	52.77 ± 2.75	**20.02 ± 2.58**	43.87 ± 2.25
Ours Improvement	+0.33	+1.36	**+2.21**	+1.52

5.2.2 Comparison results for IN2

Table 3 compares the results of IN2 and baselines. It an be seen that our Finetune-CBM already outperforms existing exemplar-free methods in balanced average accuracy $\bar{A}_T$ with often better balanced average forgetting $\bar{F}_T$, which indicates the impact of CBM in continual learning. Notably, our IN2 even has better performance on both metrics by up to 0.8% in $\bar{A}_T$ and 9.1% in $\bar{F}_T$. Additionally, combining IN2 with exemplar-based

methods can further yields more improved performance for the exemplar-based methods by up to 6.7% in $\bar{A}_T$ and 7.3% in $\bar{F}_T$. However, the trade-off between interpretability and accuracy causes a minor performance drop for MIR. CBM transforms a neural network's architecture into a more interpretable one, which causes a slight decrease in accuracy as LF-CBM (Oikarinen et al., 2023) and Post-hoc CBM (Yuksekgonul et al., 2022) shows. However, IN2 increases interpretability significantly compared with the previous continual learning methods. When remove duplicate concepts in concept set expansion 4.2, both $\bar{A}_T$ and $\bar{F}_T$ are worse than original IN2, but still better than the baselines in $\bar{F}_T$ with similar $\bar{A}_T$. Since the same text concepts can represent different visual concepts, as demonstrated in Appendix C.3, adding duplicate concepts help IN2 achieves better performance.

Table 3: Accuracy comparison for IN2. All models are pre-trained on the Place365 dataset Zhou et al. (2017). ↑ means larger values are better, while ↓ means smaller values are better. Underline means the strongest baseline, and **boldface** means the best number. In the **Ours Improvement** rows, +/- measures our best number minus the strongest baseline, and the value is in blue if our improvement is statistically significant. Our methods clearly outperform the baselines on both $\bar{A}_T$ and $\bar{F}_T$.

	CIFAR-100, 5T		TinyImagenet, 5T	
	$\bar{A}_T \uparrow$	$\bar{F}_T \downarrow$	$\bar{A}_T \uparrow$	$\bar{F}_T \downarrow$
Exemplar-free baselines				
Finetune	22.68 ± 0.88	75.69 ± 2.25	20.50 ± 0.45	66.52 ± 2.10
EWC	22.20 ± 1.56	74.93 ± 2.34	19.68 ± 1.82	65.26 ± 2.54
SI	22.70 ± 1.20	74.44 ± 2.45	18.87 ± 1.71	62.44 ± 0.68
LwF	24.20 ± 2.29	74.41 ± 3.33	20.48 ± 2.36	64.17 ± 3.08
Adam-NSCL	23.37 ± 2.14	53.87 ± 3.19	20.17 ± 2.04	58.28 ± 3.02
Ours				
Finetune-CBM	**24.99 ± 0.79**	59.29 ± 1.40	21.13 ± 1.66	61.57 ± 1.42
IN2-remove	23.21 ± 0.77	52.41 ± 1.37	20.10 ± 0.43	52.95 ± 1.05
IN2	24.25 ± 0.86	**47.62 ± 1.52**	**21.30 ± 1.55**	**49.11 ± 1.74**
Ours Improvement	+0.79	**+6.25**	+0.80	**+9.17**
Exemplar-based baselines				
GEM	24.27 ± 1.57	74.28 ± 2.54	10.54 ± 0.73	41.49 ± 1.62
Ours				
IN2-GEM	**25.41 ± 2.06**	**66.91 ± 2.16**	**12.14 ± 0.53**	**38.23 ± 0.42**
Ours Improvement	+1.14	**+7.37**	**+1.60**	**+3.26**
Exemplar-based baselines				
MIR	24.32 ± 2.09	61.22 ± 1.69	11.58 ± 2.08	**44.17 ± 2.06**
Ours				
IN2-MIR	**31.03 ± 2.23**	**60.39 ± 1.06**	**14.86 ± 1.10**	46.24 ± 2.81
Ours Improvement	**+6.71**	+0.83	**+3.28**	-2.07

Remark. Our method, IG-CL and IN2, introduces interpretability to continual learning for the first time. While achieving superior performance on two standard metrics compared to baselines, it's important to emphasize that our primary goal extends beyond mere performance enhancement. Our approach may sometimes yield accuracy similar or comparable to existing methods, yet it stands out by significantly boosting interpretability. This innovation marks a pivotal step in making continual learning not just more effective, but also more understandable.

5.3 Discussion on Concept Evolution

In this section, we visualize the learned concept to give more insights on the proposed IG-CL and IN2.

IG-CL. For IG-CL, we study the evolution of the concepts represented by neurons as we train across different tasks. We analyze the case which we group similar classes into the same task, so we can recognize which task a concept belongs to easier. For CIFAR-100 and TinyImagenet, the class distributions are in appendix D.3. We try to maximize the diversity between tasks, which makes tasks share less concepts and become more challenging in continuous learning regime. First, we use CLIP-Dissect (Oikarinen & Weng, 2022) to analyse how many units are still detecting the same concept after learning a new task. The results are in Figure 1 and Table 4. The values are in Table 5 in Appendix A.1. Compared with existing methods, our method has better ability to retain knowledge of concepts, with by up to 62.5% improvement in the preserved ratio

Table 4: Concept evolution for IG-CL in freeze-all implementation. We analyse the concept evolution in the layer 4 of ResNet18. The blue concept means the concept is related to the current task, while the green concept means it is unrelated. "x" stands for non-interpretable units. The results show that IG-CL can preserve the concepts from previous classes.

TinyImagenet, 5T					
	task 1	task 2	task 3	task 4	task 5
Classes	Big objects	Human-made small objects	Big animals & Natural scenes	Small animals & Sea animals	Food & Clothes & Others
Unit 85	x	Kitchen	Kitchen	Kitchen	Kitchen
Unit 123	x	Bedroom	Bedroom	Bedroom	Bedroom
Unit 129	Bus	Bus	Bus	Bus	Bus
CIFAR-100, 5T					
	task 1	task 2	task 3	task 4	task 5
Classes	Small animals & Sea animals	Natural scenes & Plants	Big animals	Big objects	Others
Unit 307	x	Kitchen	Kitchen	x	x
Unit 310	x	x	x	Highway	Highway

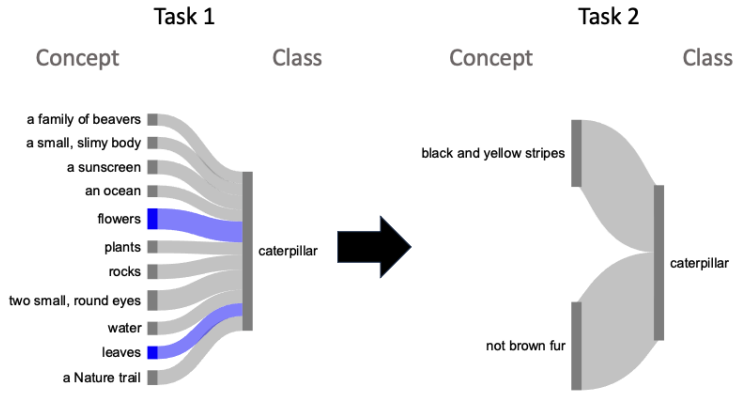

(a) Finetune-CBM

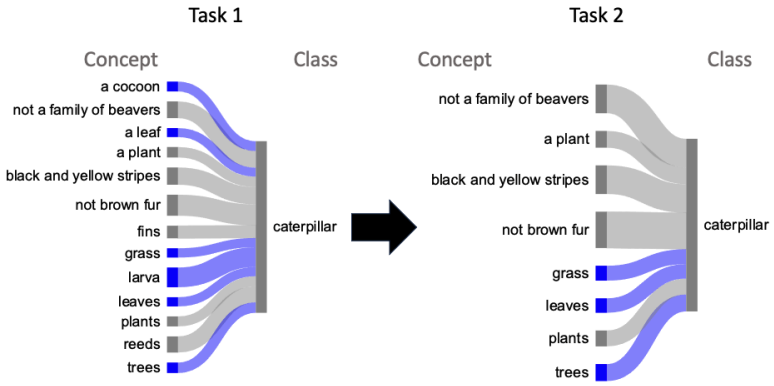

(b) IN2

Figure 5: Final weight visualization for random classes in (a) Finetune-CBM and (b) IN2 trained on CIFAR-100 under 5-tasks scenario. For class "caterpillar"from task 1, we show its significant weight (> 0.16) after training on task 1 and task 2. Concepts generated from the caterpillar class itself are colored blue, and other concepts from task 1 are colored gray. The class distribution is in Table 39. We can see IN2 keeps a similar final layer while Finetune-CBM loses most significant weights.

as Table 5 shows. We also do a case study to understand how well our method preserves the concept units from the previous tasks. Table 4 shows results for some example neurons. Some concepts are preserved after learning unrelated new tasks, which gives us insight on how our method helps avoid catastrophic forgetting. As Table 2 shows, IG-CL outperforms baselines by up to 1.3% in forgetting metric $\bar{F}_T$.

IN2. For IN2, we also studied the evolution of concepts across different tasks. Figure 5 shows an example for CIFAR-100 under 5-tasks scenario, with more results in Appendix A.2. As discussed in the previous section that though our Fine-tune CBM results is already better than many Exemplary-free baselines, our IN2 is even better than Fine-tune CBM, especially on $\bar{F}_T$, with up to 12.4% improvement. This can be seen in Figure 5 that IN2 is much better at retaining and using knowledge of concepts learned from previous tasks, which is the key to help to combat against catastrophic forgetting. As Table 3 shows, IN2 outperforms baselines by up to 9.1% in forgetting metric $\bar{F}_T$.

5.4 Ablation Studies

To understand the contributions of IG-CL and IN2's continual learning abilities, we do ablation studies in Appendix B.1 to analysis each part of the methods. The experiment results show that combining all ideas in Section 3 and Section 4 leads to best performances in continual learning. For IG-CL, freezing concept subnetworks improves $\bar{A}_T$ by up to 3.1% and 4.8% in $\bar{F}_T$, and regularizing W_F improves $\bar{A}_T$ by up to 3.6% and 7.3% in $\bar{F}_T$. For IN2, regularizing W_F improves $\bar{A}_T$ by up to 6.2% and 2.5% in $\bar{F}_T$.

6 Conclusion

In this work, we introduced two novel interpretable continual learning frameworks: **Interpretability Guided Continual Learning** (IG-CL) and **Intrinsically Interpretable Neural Network** (IN2). The main goal of our research is to integrate interpretability into continual learning, enhancing transparency and control throughout the learning process. Although our primary focus is not on performance enhancement, our findings demonstrate that IG-CL and IN2 frequently outperform existing methods. Specifically, these frameworks improve upon previous continual learning methods by up to 1.4% in average incremental accuracy, and up to 9.1% in average incremental forgetting. Furthermore, they effectively preserve learned knowledge without the need for storing past data. The clear and interpretable nature of IG-CL and IN2 sets a strong foundation for future advancements in the field of continual learning.

Broader Impacts

The improvement of mitigating forgetting by controlling concepts in models might have some potential negative impact in terms of privacy. For example, if an adversary only has access to model checkpoints but not model's training data, they can analyse the concept units in the model. This will give the attacker some information about how the model was trained, and may allow them to extract some private information from the models without access to training data.

References

Rahaf Aljundi, Francesca Babiloni, Mohamed Elhoseiny, Marcus Rohrbach, and Tinne Tuytelaars. Memory aware synapses: Learning what (not) to forget. In *Proceedings of the European conference on computer vision (ECCV)*, pp. 139–154, 2018.

Rahaf Aljundi, Lucas Caccia, Eugene Belilovsky, Massimo Caccia, Min Lin, Laurent Charlin, and Tinne Tuytelaars. Online continual learning with maximally interfered retrieval. *arXiv preprint arXiv:1908.04742*, 2019.

David Bau, Bolei Zhou, Aditya Khosla, Aude Oliva, and Antonio Torralba. Network dissection: Quantifying interpretability of deep visual representations. In *Computer Vision and Pattern Recognition*, 2017.

David Bau, Jun-Yan Zhu, Hendrik Strobelt, Agata Lapedriza, Bolei Zhou, and Antonio Torralba. Understanding the role of individual units in a deep neural network. *Proceedings of the National Academy of*

Sciences, 2020. ISSN 0027-8424. doi: 10.1073/pnas.1907375117. URL https://www.pnas.org/content/early/2020/08/31/1907375117.

Tom Brown, Benjamin Mann, Nick Ryder, Melanie Subbiah, Jared D Kaplan, Prafulla Dhariwal, Arvind Neelakantan, Pranav Shyam, Girish Sastry, Amanda Askell, et al. Language models are few-shot learners. *Advances in neural information processing systems*, 33:1877–1901, 2020.

Pietro Buzzega, Matteo Boschini, Angelo Porrello, Davide Abati, and Simone Calderara. Dark experience for general continual learning: a strong, simple baseline. *Advances in neural information processing systems*, 33:15920–15930, 2020.

Lucas Caccia, Rahaf Aljundi, Nader Asadi, Tinne Tuytelaars, Joelle Pineau, and Eugene Belilovsky. New insights on reducing abrupt representation change in online continual learning. *arXiv preprint arXiv:2104.05025*, 2021.

Massimo Caccia, Pau Rodriguez, Oleksiy Ostapenko, Fabrice Normandin, Min Lin, Lucas Page-Caccia, Issam Hadj Laradji, Irina Rish, Alexandre Lacoste, David Vázquez, et al. Online fast adaptation and knowledge accumulation (osaka): a new approach to continual learning. *Advances in Neural Information Processing Systems*, 33:16532–16545, 2020.

Xinyuan Cao, Weiyang Liu, and Santosh Vempala. Provable lifelong learning of representations. In *International Conference on Artificial Intelligence and Statistics*, pp. 6334–6356. PMLR, 2022.

Antonio Carta, Joost Van de Weijer, et al. Improving online continual learning performance and stability with temporal ensembles. *arXiv preprint arXiv:2306.16817*, 2023.

Francisco M Castro, Manuel J Marín-Jiménez, Nicolás Guil, Cordelia Schmid, and Karteek Alahari. End-to-end incremental learning. In *Proceedings of the European conference on computer vision (ECCV)*, pp. 233–248, 2018.

Arslan Chaudhry, Puneet K Dokania, Thalaiyasingam Ajanthan, and Philip HS Torr. Riemannian walk for incremental learning: Understanding forgetting and intransigence. In *Proceedings of the European conference on computer vision (ECCV)*, pp. 532–547, 2018a.

Arslan Chaudhry, Marc'Aurelio Ranzato, Marcus Rohrbach, and Mohamed Elhoseiny. Efficient lifelong learning with a-gem. *arXiv preprint arXiv:1812.00420*, 2018b.

Xi Chen, Christos Papadimitriou, and Binghui Peng. Memory bounds for continual learning. In *2022 IEEE 63rd Annual Symposium on Foundations of Computer Science (FOCS)*, pp. 519–530. IEEE, 2022.

Matthias De Lange, Rahaf Aljundi, Marc Masana, Sarah Parisot, Xu Jia, Aleš Leonardis, Gregory Slabaugh, and Tinne Tuytelaars. A continual learning survey: Defying forgetting in classification tasks. *IEEE transactions on pattern analysis and machine intelligence*, 44(7):3366–3385, 2021.

Prithviraj Dhar, Rajat Vikram Singh, Kuan-Chuan Peng, Ziyan Wu, and Rama Chellappa. Learning without memorizing. In *Proceedings of the IEEE/CVF conference on computer vision and pattern recognition*, pp. 5138–5146, 2019.

Yiduo Guo, Bing Liu, and Dongyan Zhao. Online continual learning through mutual information maximization. In *International Conference on Machine Learning*, pp. 8109–8126. PMLR, 2022.

Kaiming He, Xiangyu Zhang, Shaoqing Ren, and Jian Sun. Deep residual learning for image recognition. In *Proceedings of the IEEE conference on computer vision and pattern recognition*, pp. 770–778, 2016.

Evan Hernandez, Sarah Schwettmann, David Bau, Teona Bagashvili, Antonio Torralba, and Jacob Andreas. Natural language descriptions of deep visual features. In *International Conference on Learning Representations*, 2022.

Saihui Hou, Xinyu Pan, Chen Change Loy, Zilei Wang, and Dahua Lin. Learning a unified classifier incrementally via rebalancing. In *Proceedings of the IEEE/CVF conference on Computer Vision and Pattern Recognition*, pp. 831–839, 2019.

Linmei Hu, Tianchi Yang, Luhao Zhang, Wanjun Zhong, Duyu Tang, Chuan Shi, Nan Duan, and Ming Zhou. Compare to the knowledge: Graph neural fake news detection with external knowledge. In *Proceedings of the 59th Annual Meeting of the Association for Computational Linguistics and the 11th International Joint Conference on Natural Language Processing (Volume 1: Long Papers)*, pp. 754–763, 2021.

Wenpeng Hu, Zhou Lin, Bing Liu, Chongyang Tao, Zhengwei Tao Tao, Dongyan Zhao, Jinwen Ma, and Rui Yan. Overcoming catastrophic forgetting for continual learning via model adaptation. In *International conference on learning representations*, 2019.

Heechul Jung, Jeongwoo Ju, Minju Jung, and Junmo Kim. Less-forgetting learning in deep neural networks. *arXiv preprint arXiv:1607.00122*, 2016.

Gyuhak Kim, Changnan Xiao, Tatsuya Konishi, Zixuan Ke, and Bing Liu. A theoretical study on solving continual learning. *Advances in Neural Information Processing Systems*, 35:5065–5079, 2022.

James Kirkpatrick, Razvan Pascanu, Neil Rabinowitz, Joel Veness, Guillaume Desjardins, Andrei A Rusu, Kieran Milan, John Quan, Tiago Ramalho, Agnieszka Grabska-Barwinska, et al. Overcoming catastrophic forgetting in neural networks. *Proceedings of the national academy of sciences*, 114(13):3521–3526, 2017.

Hyunseo Koh, Dahyun Kim, Jung-Woo Ha, and Jonghyun Choi. Online continual learning on class incremental blurry task configuration with anytime inference. *arXiv preprint arXiv:2110.10031*, 2021.

Pang Wei Koh, Thao Nguyen, Yew Siang Tang, Stephen Mussmann, Emma Pierson, Been Kim, and Percy Liang. Concept bottleneck models. In *International Conference on Machine Learning*, pp. 5338–5348. PMLR, 2020.

Alex Krizhevsky, Geoffrey Hinton, et al. Learning multiple layers of features from tiny images. 2009.

Ya Le and Xuan Yang. Tiny imagenet visual recognition challenge. *CS 231N*, 7(7):3, 2015.

Kibok Lee, Kimin Lee, Jinwoo Shin, and Honglak Lee. Overcoming catastrophic forgetting with unlabeled data in the wild. In *Proceedings of the IEEE/CVF International Conference on Computer Vision*, pp. 312–321, 2019.

Sang-Woo Lee, Jin-Hwa Kim, Jaehyun Jun, Jung-Woo Ha, and Byoung-Tak Zhang. Overcoming catastrophic forgetting by incremental moment matching. *Advances in neural information processing systems*, 30, 2017.

Xilai Li, Yingbo Zhou, Tianfu Wu, Richard Socher, and Caiming Xiong. Learn to grow: A continual structure learning framework for overcoming catastrophic forgetting. In *International Conference on Machine Learning*, pp. 3925–3934. PMLR, 2019.

Zhizhong Li and Derek Hoiem. Learning without forgetting. *IEEE transactions on pattern analysis and machine intelligence*, 40(12):2935–2947, 2017.

Yaoyao Liu, Bernt Schiele, and Qianru Sun. Adaptive aggregation networks for class-incremental learning. In *Proceedings of the IEEE/CVF conference on Computer Vision and Pattern Recognition*, pp. 2544–2553, 2021.

Vincenzo Lomonaco, Lorenzo Pellegrini, Andrea Cossu, Antonio Carta, Gabriele Graffieti, Tyler L Hayes, Matthias De Lange, Marc Masana, Jary Pomponi, Gido M Van de Ven, et al. Avalanche: an end-to-end library for continual learning. In *Proceedings of the IEEE/CVF Conference on Computer Vision and Pattern Recognition*, pp. 3600–3610, 2021.

David Lopez-Paz and Marc'Aurelio Ranzato. Gradient episodic memory for continual learning. *Advances in neural information processing systems*, 30, 2017.

Max Losch, Mario Fritz, and Bernt Schiele. Interpretability beyond classification output: Semantic bottleneck networks. *arXiv preprint arXiv:1907.10882*, 2019.

Emanuele Marconato, Gianpaolo Bontempo, Elisa Ficarra, Simone Calderara, Andrea Passerini, and Stefano Teso. Neuro symbolic continual learning: Knowledge, reasoning shortcuts and concept rehearsal. *arXiv preprint arXiv:2302.01242*, 2023.

Seyed Iman Mirzadeh, Arslan Chaudhry, Dong Yin, Huiyi Hu, Razvan Pascanu, Dilan Gorur, and Mehrdad Farajtabar. Wide neural networks forget less catastrophically. In *International Conference on Machine Learning*, pp. 15699–15717. PMLR, 2022a.

Seyed Iman Mirzadeh, Arslan Chaudhry, Dong Yin, Timothy Nguyen, Razvan Pascanu, Dilan Gorur, and Mehrdad Farajtabar. Architecture matters in continual learning. *arXiv preprint arXiv:2202.00275*, 2022b.

Jesse Mu and Jacob Andreas. Compositional explanations of neurons. *Advances in Neural Information Processing Systems*, 33:17153–17163, 2020.

Tuomas Oikarinen and Tsui-Wei Weng. Clip-dissect: Automatic description of neuron representations in deep vision networks. *arXiv preprint arXiv:2204.10965*, 2022.

Tuomas Oikarinen, Subhro Das, Lam M Nguyen, and Tsui-Wei Weng. Label-free concept bottleneck models. In *International Conference on Learning Representations*, 2023.

Binghui Peng and Andrej Risteski. Continual learning: a feature extraction formalization, an efficient algorithm, and fundamental obstructions. *arXiv preprint arXiv:2203.14383*, 2022.

Liangzu Peng, Paris V Giampouras, and René Vidal. The ideal continual learner: An agent that never forgets. *arXiv preprint arXiv:2305.00316*, 2023.

Anastasia Pentina and Ruth Urner. Lifelong learning with weighted majority votes. *Advances in Neural Information Processing Systems*, 29, 2016.

Alec Radford, Jong Wook Kim, Chris Hallacy, Aditya Ramesh, Gabriel Goh, Sandhini Agarwal, Girish Sastry, Amanda Askell, Pamela Mishkin, Jack Clark, et al. Learning transferable visual models from natural language supervision. In *International conference on machine learning*, pp. 8748–8763. PMLR, 2021.

Sylvestre-Alvise Rebuffi, Alexander Kolesnikov, Georg Sperl, and Christoph H Lampert. icarl: Incremental classifier and representation learning. In *Proceedings of the IEEE conference on Computer Vision and Pattern Recognition*, pp. 2001–2010, 2017.

Matthew Riemer, Ignacio Cases, Robert Ajemian, Miao Liu, Irina Rish, Yuhai Tu, and Gerald Tesauro. Learning to learn without forgetting by maximizing transfer and minimizing interference. *arXiv preprint arXiv:1810.11910*, 2018.

David Rolnick, Arun Ahuja, Jonathan Schwarz, Timothy Lillicrap, and Gregory Wayne. Experience replay for continual learning. *Advances in Neural Information Processing Systems*, 32, 2019.

Olga Russakovsky, Jia Deng, Hao Su, Jonathan Krause, Sanjeev Satheesh, Sean Ma, Zhiheng Huang, Andrej Karpathy, Aditya Khosla, Michael Bernstein, Alexander C. Berg, and Li Fei-Fei. ImageNet Large Scale Visual Recognition Challenge. *International Journal of Computer Vision (IJCV)*, 115(3):211–252, 2015. doi: 10.1007/s11263-015-0816-y.

Andrei A Rusu, Neil C Rabinowitz, Guillaume Desjardins, Hubert Soyer, James Kirkpatrick, Koray Kavukcuoglu, Razvan Pascanu, and Raia Hadsell. Progressive neural networks. *arXiv preprint arXiv:1606.04671*, 2016.

Paul Ruvolo and Eric Eaton. Ella: An efficient lifelong learning algorithm. In *International conference on machine learning*, pp. 507–515. PMLR, 2013.

Dawid Rymarczyk, Joost van de Weijer, Bartosz Zieliński, and Bartlomiej Twardowski. Icicle: Interpretable class incremental continual learning. In *Proceedings of the IEEE/CVF International Conference on Computer Vision*, pp. 1887–1898, 2023.

Hassan Sajjad, Nadir Durrani, and Fahim Dalvi. Neuron-level interpretation of deep nlp models: A survey. *Transactions of the Association for Computational Linguistics*, 10:1285–1303, 2022.

Jonathan Schwarz, Wojciech Czarnecki, Jelena Luketina, Agnieszka Grabska-Barwinska, Yee Whye Teh, Razvan Pascanu, and Raia Hadsell. Progress & compress: A scalable framework for continual learning. In *International conference on machine learning*, pp. 4528–4537. PMLR, 2018.

Joan Serra, Didac Suris, Marius Miron, and Alexandros Karatzoglou. Overcoming catastrophic forgetting with hard attention to the task. In *International Conference on Machine Learning*, pp. 4548–4557. PMLR, 2018.

Gido M van de Ven, Tinne Tuytelaars, and Andreas S Tolias. Three types of incremental learning. *Nature Machine Intelligence*, pp. 1–13, 2022.

Catherine Wah, Steve Branson, Peter Welinder, Pietro Perona, and Serge Belongie. The caltech-ucsd birds-200-2011 dataset. 2011.

Liyuan Wang, Xingxing Zhang, Kuo Yang, Longhui Yu, Chongxuan Li, Lanqing Hong, Shifeng Zhang, Zhenguo Li, Yi Zhong, and Jun Zhu. Memory replay with data compression for continual learning. *arXiv preprint arXiv:2202.06592*, 2022.

Shipeng Wang, Xiaorong Li, Jian Sun, and Zongben Xu. Training networks in null space of feature covariance for continual learning. In *Proceedings of the IEEE/CVF conference on Computer Vision and Pattern Recognition*, pp. 184–193, 2021.

Yue Wu, Yinpeng Chen, Lijuan Wang, Yuancheng Ye, Zicheng Liu, Yandong Guo, and Yun Fu. Large scale incremental learning. In *Proceedings of the IEEE/CVF Conference on Computer Vision and Pattern Recognition*, pp. 374–382, 2019.

Ju Xu and Zhanxing Zhu. Reinforced continual learning. *Advances in Neural Information Processing Systems*, 31, 2018.

An Yan, Yu Wang, Yiwu Zhong, Chengyu Dong, Zexue He, Yujie Lu, William Yang Wang, Jingbo Shang, and Julian McAuley. Learning concise and descriptive attributes for visual recognition. In *Proceedings of the IEEE/CVF International Conference on Computer Vision*, pp. 3090–3100, 2023.

Shipeng Yan, Jiangwei Xie, and Xuming He. Der: Dynamically expandable representation for class incremental learning. In *Proceedings of the IEEE/CVF Conference on Computer Vision and Pattern Recognition*, pp. 3014–3023, 2021.

Sin-Han Yang, Chung-Chi Chen, Hen-Hsen Huang, and Hsin-Hsi Chen. Entity-aware dual co-attention network for fake news detection. *arXiv preprint arXiv:2302.03475*, 2023a.

Yue Yang, Artemis Panagopoulou, Shenghao Zhou, Daniel Jin, Chris Callison-Burch, and Mark Yatskar. Language in a bottle: Language model guided concept bottlenecks for interpretable image classification. In *Proceedings of the IEEE/CVF Conference on Computer Vision and Pattern Recognition*, pp. 19187–19197, 2023b.

Haiyan Yin, Ping Li, et al. Mitigating forgetting in online continual learning with neuron calibration. *Advances in Neural Information Processing Systems*, 34:10260–10272, 2021.

Jaehong Yoon, Eunho Yang, Jeongtae Lee, and Sung Ju Hwang. Lifelong learning with dynamically expandable networks. *arXiv preprint arXiv:1708.01547*, 2017.

Mert Yuksekgonul, Maggie Wang, and James Zou. Post-hoc concept bottleneck models. *arXiv preprint arXiv:2205.15480*, 2022.

Friedemann Zenke, Ben Poole, and Surya Ganguli. Continual learning through synaptic intelligence. In *International conference on machine learning*, pp. 3987–3995. PMLR, 2017.

Bolei Zhou, Agata Lapedriza, Aditya Khosla, Aude Oliva, and Antonio Torralba. Places: A 10 million image database for scene recognition. *IEEE Transactions on Pattern Analysis and Machine Intelligence*, 2017.

Bolei Zhou, Yiyou Sun, David Bau, and Antonio Torralba. Interpretable basis decomposition for visual explanation. In *Proceedings of the European Conference on Computer Vision (ECCV)*, pp. 119–134, 2018.

Da-Wei Zhou, Qi-Wei Wang, Zhi-Hong Qi, Han-Jia Ye, De-Chuan Zhan, and Ziwei Liu. Deep class-incremental learning: A survey. *arXiv preprint arXiv:2302.03648*, 2023.

Kai Zhu, Wei Zhai, Yang Cao, Jiebo Luo, and Zheng-Jun Zha. Self-sustaining representation expansion for non-exemplar class-incremental learning. In *Proceedings of the IEEE/CVF Conference on Computer Vision and Pattern Recognition*, pp. 9296–9305, 2022.

Appendix Outline

In this section we provide a brief overview of the Appendix contents.

- A:Interpretability Analysis
  - A.1: IG-CL's Concept Evolution
  - A.2: Discussion of Concept Evolution for IN2
- B: Additional Experiments
  - B.1: Ablation Study
  - B.2: Ablation on IN2 Sparsity
  - B.3: More 5 task Results
  - B.4: 10, 20 tasks Experiment Results
  - B.5: Comparison with SSRE, DEN and ICICLE
  - B.6: Foward Transfer Metric
  - B.7: Experiment Results on ImageNet-10
- C: Further Analysis and Details
  - C.1: Computational Efficiency
  - C.2: **Interpretability Guided Continual Learning** Algorithm
  - C.3: Details of IG-CL and IN2
- D: Others
  - D.1: Experiment Setup and Details
  - D.2: Previous Continual Learning Methods
  - D.3: Class Distribution

A Interpretability Analysis

A.1 IG-CL's Concept Evolution

Figure 1 and Table 4 show the IG-CL's concept evolution when grouping similar classes together. The analysis is in Section 5.3. Meanwhile, we visualize the classification head's weight for IG-CL in Figure 6. IG-CL can preserve classes' related concepts contribution to prediction. Compared with IN2 that analyzed in Figure 5, IG-CL's perserved concepts are more general and less task-specific since IG-CL can not control the emergence and types of related concepts.

Besides grouping similar classes into the same task, we also analyse the cases where class labels are distributed randomly. Following the same procedure as in section 5.3, we analyse how many units are still detecting the same concept after learning a new task. The average results for three datasets are in Table 6. Similar to Table 5, our methods outperform existing methods to retain knowledge of concepts learned from previous tasks. In general the concepts are more stable in random class distribution since different tasks might share more overlapped concepts.

Table 5: The ratio of units that still detect the same concepts they detected in the last task. Tasks' classes are in Appendix D.3. Underline means the strongest baseline, and **boldface** means the best number. Our methods outperform existing exemplar-free methods for preserving concepts, and are even better than exemplar-based methods without replaying buffer.

Method	CIFAR100, 5T				TinyImagenet, 5T			
	Task 2	Task 3	Task 4	Task 5	Task 2	Task 3	Task 4	Task 5
Exemplar-free baselines								
Finetune	0	0	0	0	0	0	0	0.086
EWC	0	0	0	0	0	0.030	0.037	0
SI	0	0	0	0	0.028	0.191	0.200	0.250
LwF	0.019	0.011	0.176	0	0.114	0.191	0.393	0.365
Exemplar-based baselines								
GEM	0	0.125	0.076	0.153	0	0	0	0
MIR	0	0	0	0.250	0.028	0	0	0
Ours								
IG-CL-freeze-all (no replay)	**0.500**	**0.500**	0.571	**0.700**	**0.739**	**0.771**	**0.812**	**0.812**
IG-CL-freeze-part (no replay)	0.125	0.133	**0.727**	0.695	0.515	0.488	0.544	0.666

Table 6: The ratio of units which still detect the same concepts they detected in the last task for CIFAR-10 and CIFAR-100. Class labels are distributed randomly, and the results are average over three runs. Underline means the strongest baseline, and **boldface** means the best number. Our methods outperform the existing works for preserving learned concepts.

Method	CIFAR10, 5T				CIFAR100, 5T				TinyImagenet, 5T			
	Task 2	Task 3	Task 4	Task 5	Task 2	Task 3	Task 4	Task 5	Task 2	Task 3	Task 4	Task 5
Exemplar-free baselines												
Finetune	0	0	0	0	0.020	0.005	0.010	0	0	0.010	0	0.030
EWC	0	0	0	0	0.065	0.010	0	0	0.030	0.015	0	0.010
SI	0	0	0	0	0	0	0	0	0.011	0	0	0
LwF	0	0	0	0	0.020	0.030	0	0	0.015	0	0	0
Exemplar-based baselines												
GEM	0	0.031	0	0	0.138	0.043	0.006	0.023	0	0.041	0.012	0.029
MIR	0	0	0	0	0.028	0	0.050	0.052	0	0	0	0
Ours												
IG-CL-freeze-all	**0.052**	**0.500**	**0.111**	**0.200**	**0.578**	**0.636**	**0.782**	0.741	**0.724**	**0.833**	**0.741**	0.812
IG-CL-freeze-part	0.023	0.450	0.090	0.150	0.210	0.466	0.687	**0.869**	0.586	0.739	0.666	**0.821**

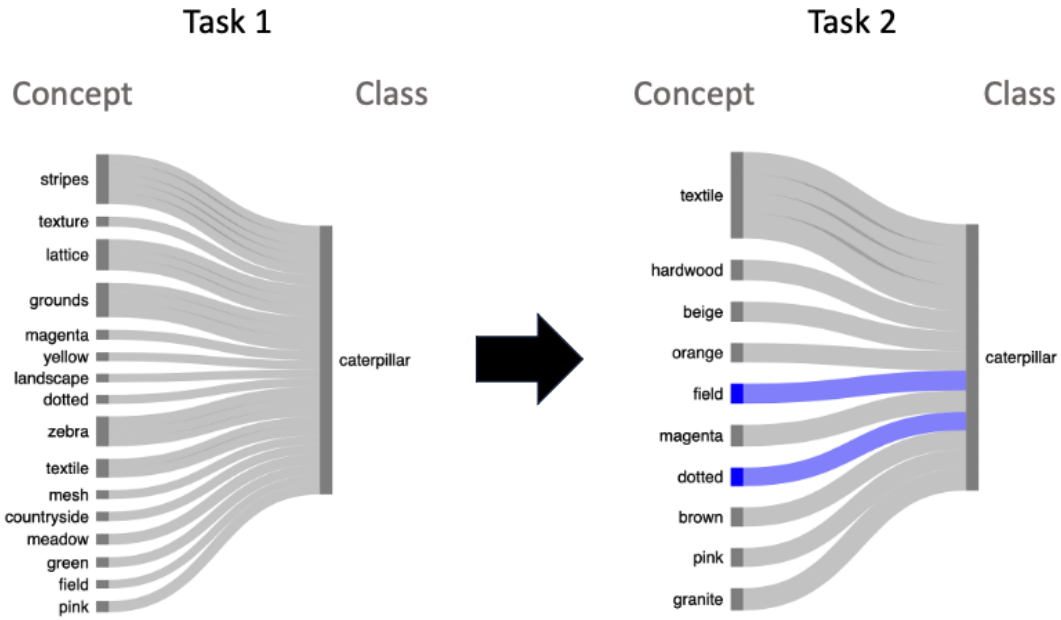

(a) caterpillar

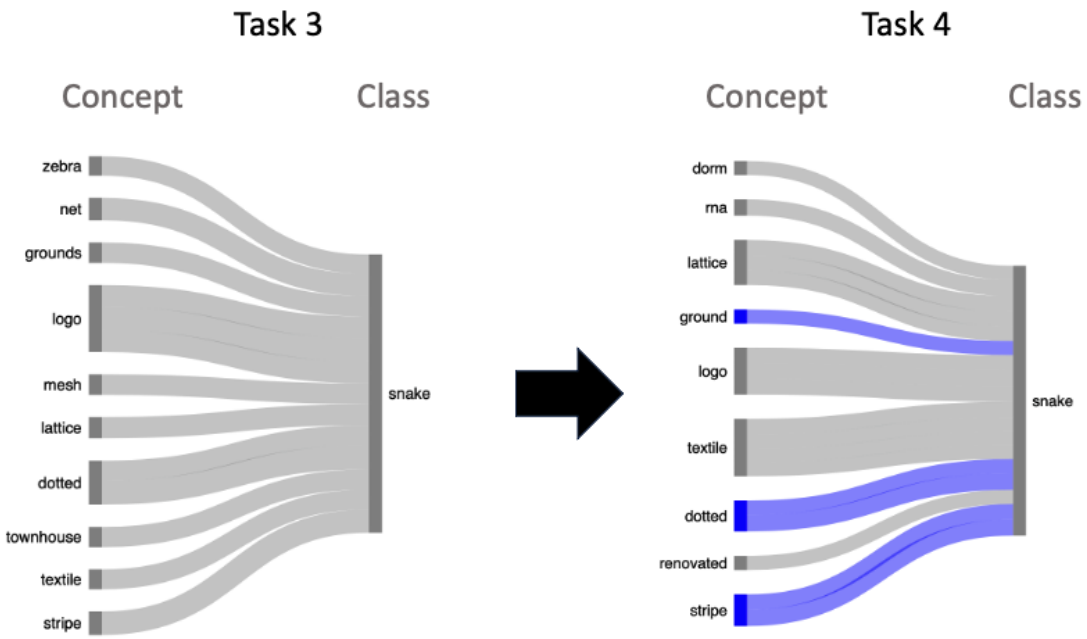

(b) snake

Figure 6: Final weight visualization for random classes in IG-CL on CIFAR-100 under 5-tasks scenario. For class "caterpillar" from task 1, we show its significant weight (> 0.05) after training on task 1 and task 2. For class "snake" from task 3, we show its significant weight after training on task 3 and task 4. Concepts related to caterpillar, and preserved from task 1 to task 2 are marked in blue. Same for concepts related to snake and preserved from task 3 to task 4. The class distribution is in Table 39. We can see IG-CL has ability to preserve related concepts' appearance and contribution.

A.2 Discussion of Concept Evolution for IN2

In this section, we study the evolution of the concepts represented by neurons and final layer weights as we train IN2 across different tasks under 5-tasks scenario. We analyse a classes' final layer weights after learning its task, and after learning a new task. We visualize the final layer weights of Finetune-CBM and IN2 by Sankey diagrams, only including weights with absolute value greater than predefined threshold. Negative weights are reported as "NOT {concept}". The visualization for random classes in CIFAR-100 are in the main text Figure 5. The visualizations for random classes in other two datasets are in Figure 7 8. Compared with Finetune-CBM, we can see IN2 is much better at retaining and using knowledge of concepts learned from previous tasks. This helps explain why IN2 performs better in F_T and $\bar{F}_T$.

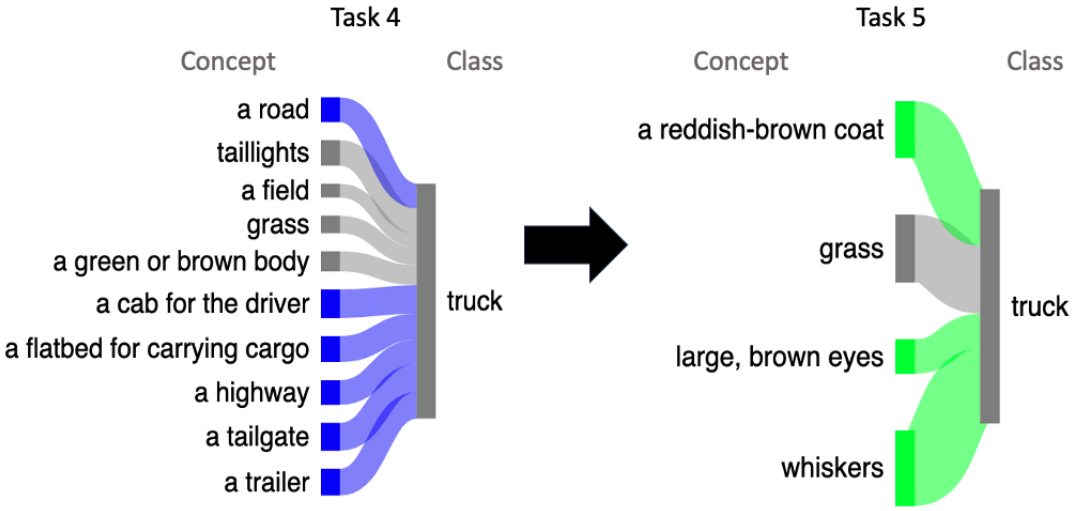

(a) Finetune-CBM

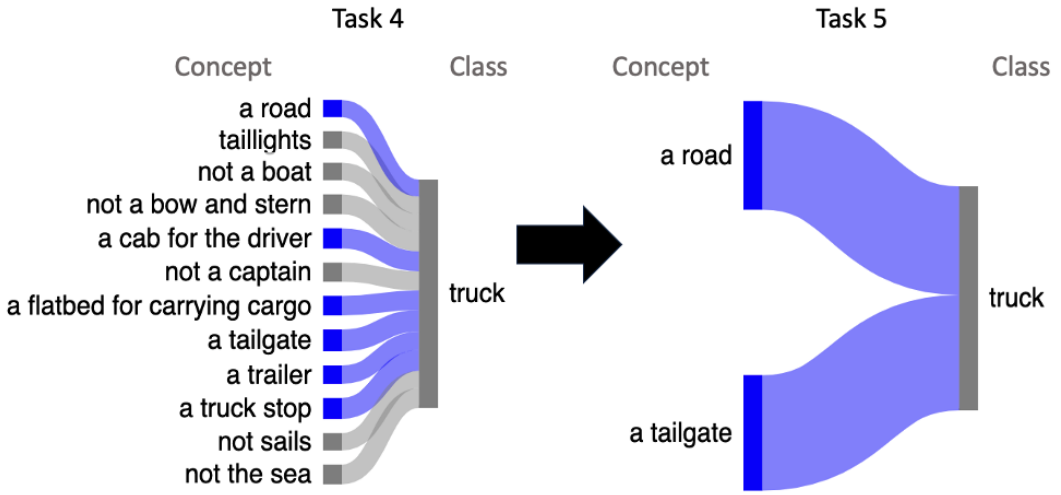

(b) IN2

Figure 7: Final weight visualization for random classes in (a) Finetune-CBM and (b) IN2 trained on CIFAR-10 under 5-tasks scenario. For class "truck" from task 4, we show its significant weight (> 0.15) after training on task 4 and task 5. Concepts generated from the truck class itself are colored blue, and other concepts from task 4 are colored gray. Concepts from task 5 are colored green. The class distribution is in Table 36. We can see both models change significantly, but IN2 keeps more concepts from original task.

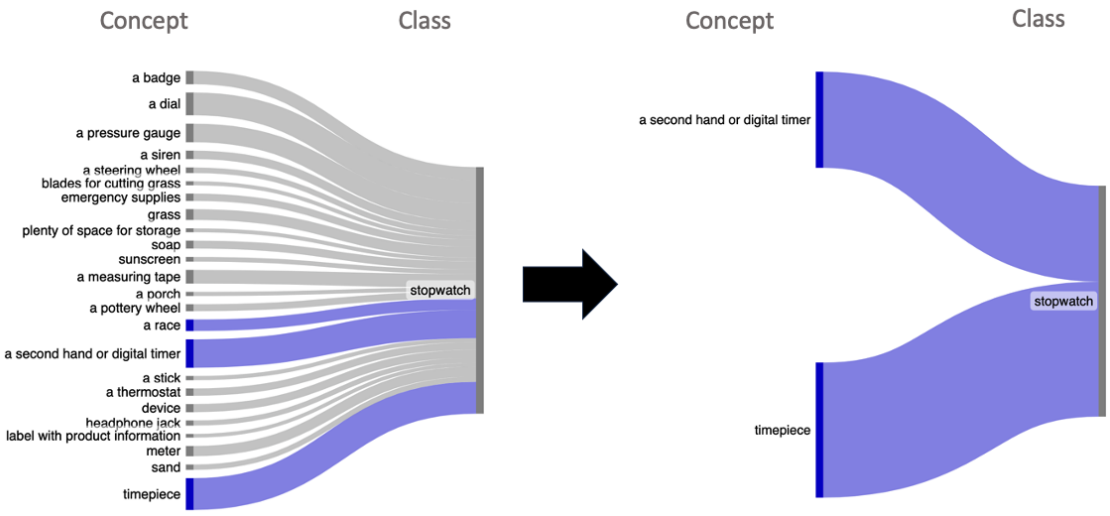

(a) Finetune-CBM

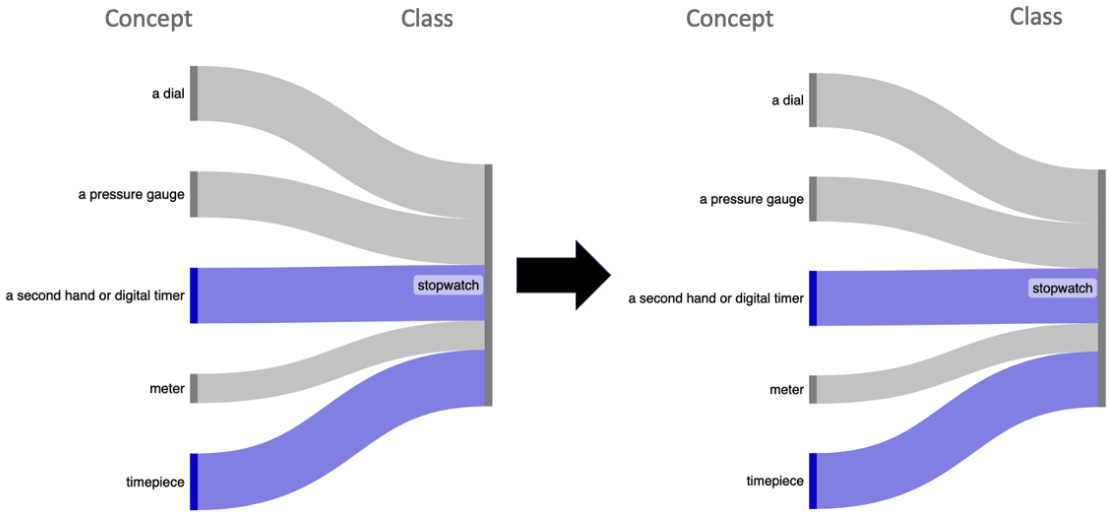

(b) IN2

Figure 8: Final weight visualization for a random class in (a) Finetune-CBM and (b) IN2 trained on TinyImageNet under 5-tasks scenario. For class "stopwatch" from task 2, we show its significant weight (> 0.05) after training on task 2 and task 3. Concepts generated from the stopwatch class itself are colored blue, and other concepts from task 2 are colored gray. The class distribution is in Table 42. We can see IN2 weights stay almost identical, while Finetune-CBM changes a lot.

B Additional Experiments

B.1 Ablation Study

Besides comparing the results with existing methods, we perform ablation study to analyze the impact of the key components in our methods. In Table 7, we compare IG-CL with (i) not freezing subnetwork in step 3, which is denoted as "IG-CL w/o freeze", and (ii) not regularizing parameter $\mathbf{W}_F$ in step 4, which is denoted as "IG-CL-freeze-all w/o reg" or "IG-CL-freeze-part w/o reg". The experiment results show that combining two of them results in less forgetting and better average accuracy. We believe it's because they are necessary to each other. If the concept units' subnetworks are not frozen, the concepts might change and the regularization term may not work. On the other hand, if the $\mathbf{W}_F$ changes when learning new tasks, then the concept units learned from previous tasks may not contribute to the final prediction.

For IN2, we do a similar ablation study with (i) not freezing previously learned concepts when learning CBL in step 2, which is denoted as "IN2 w/o freeze", and (ii) not regularizing parameter $\mathbf{W}_F$ in step 3, which is denoted as "IN2 w/o reg". The result Table 8 shows a similar result. In conclusion, these ablation studies demonstrate the importance of both freezing subnetworks and regularizing the $\mathbf{W}_F$ to achieving better performance and mitigating forgetting.

Table 7: Experiment results of IG-CL's ablation study. "IG-CL w/o freeze": not freezing subnetwork. "IG-CL-freeze-all w/o reg" and "IG-CL-freeze-part w/o reg": not regularizing parameter $\mathbf{W}_F$. ↑ means larger values are better, while ↓ means smaller values are better. Preserving two components turns out have the best performances.

	CIFAR-10, 5T		CIFAR-100, 5T		TinyImagenet, 5T	
	$\bar{A}_T \uparrow$	$\bar{F}_T \downarrow$	$\bar{A}_T \uparrow$	$\bar{F}_T \downarrow$	$\bar{A}_T \uparrow$	$\bar{F}_T \downarrow$
IG-CL w/o freeze	29.77 ± 0.12	94.76 ± 1.48	19.27 ± 2.53	60.23 ± 6.53	15.51 ± 2.14	48.26 ± 4.57
IG-CL-freeze-all w/o reg	30.13 ± 0.62	95.50 ± 1.27	19.32 ± 2.02	59.77 ± 4.99	14.56 ± 2.37	50.69 ± 3.88
IG-CL-freeze-part w/o reg	30.17 ± 0.58	95.50 ± 1.27	21.21 ± 1.65	62.04 ± 4.58	15.07 ± 2.50	51.28 ± 4.22
IG-CL-freeze-all	**31.55 ± 0.13**	**92.69 ± 0.81**	**22.37 ± 1.20**	**58.75 ± 0.26**	**18.19 ± 0.76**	**43.39 ± 0.92**
IG-CL-freeze-part	30.55 ± 0.84	94.47 ± 1.12	21.73 ± 0.79	60.51 ± 0.35	18.08 ± 0.56	46.00 ± 0.66

Table 8: Experiment results of IN2's ablation study. "IN2 w/o freeze": not freezing previous concepts. "IN2 w/o reg": not regularizing parameter $\mathbf{W}_F$. Preserving both has the best performance.

	CIFAR-10, 5T		CIFAR-100, 5T		TinyImagenet, 5T	
	$\bar{A}_T \uparrow$	$\bar{F}_T \downarrow$	$\bar{A}_T \uparrow$	$\bar{F}_T \downarrow$	$\bar{A}_T \uparrow$	$\bar{F}_T \downarrow$
IN2 w/o freeze	29.78 ± 2.45	**87.76 ± 1.07**	18.01 ± 3.42	49.50 ± 2.58	17.30 ± 2.89	51.64 ± 4.00
IN2 w/o reg	28.75 ± 1.62	91.10 ± 2.20	20.42 ± 2.68	58.72 ± 1.04	19.76 ± 2.26	62.24 ± 2.85
IN2	**32.25 ± 0.76**	88.58 ± 0.30	**24.25 ± 0.86**	**47.62 ± 1.52**	**21.30 ± 1.55**	**49.11 ± 1.74**

B.2 Ablation on IN2 Sparsity

In this section we experimented with some modifications to W_F in our CBM and report their results. In our main results for IN2 and Finetune-CBM, we used a dense final layer W_F instead of the sparse final layer used by (Oikarinen et al., 2023) as we found that to have best performance, and we are less focused on interpretable final decisions. Below we compare the results for CBM between dense W_F, and sparse W_F (-S). For the sparse W_F, we used $\lambda = 10^{-6}$ in Eq. 3. The experiment results are in Table 9. We found that dense W_F had the best performance in most cases.

Table 9: Experiment results of CBM based methods on 3 datasets. "S": sparse W_F. Dense W_F results in best performance in average.

	CIFAR-10,5T		CIFAR-100, 5T		TinyImageNet, 5T	
	$\bar{A}_T \uparrow$	$\bar{F}_T \downarrow$	$\bar{A}_T \uparrow$	$\bar{F}_T \downarrow$	$\bar{A}_T \uparrow$	$\bar{F}_T \downarrow$
Finetune-CBM	30.39 ± 0.67	93.09 ± 2.22	**24.99 ± 0.79**	59.29 ± 1.40	21.13 ± 1.66	61.57 ± 1.42
IN2	**32.25 ± 0.76**	88.58 ± 0.30	24.25 ± 0.86	47.62 ± 1.52	**21.30 ± 1.55**	49.11 ± 1.74
Finetune-CBM-S	28.84 ± 1.35	91.74 ± 2.22	20.23 ± 2.79	58.29 ± 3.12	19.50 ± 2.33	61.57 ± 2.87
IN2-S	30.11 ± 3.04	**87.58 ± 0.30**	19.20 ± 3.77	**46.62 ± 2.52**	19.50 ± 3.03	**46.11 ± 3.48**
IN2-GEM	**36.37 ± 1.74**	**44.72 ± 2.71**	**25.41 ± 2.06**	66.91 ± 2.16	**12.14 ± 0.53**	**38.23 ± 0.42**
IN2-GEM-S	36.32 ± 2.90	45.28 ± 4.17	25.40 ± 4.13	**65.21 ± 3.28**	5.32 ± 1.06	39.23 ± 0.85

B.3 More 5 task Results

In Table 10 and 11, we report A_T and F_T for CIFAR-100 and TinyImageNet, and also experiment results for CIFAR-10 in 4 metrics.

Table 10: Accuracy comparison for IG-CL. ↑ means larger values are better, while ↓ means smaller values are better. Underline means the strongest baseline, and **boldface** means the best number. In the **Ours Improvement** rows, +/- measures our best number minus the strongest baseline, and the value is in blue if our improvement is statistically significant.

	CIFAR-10, 5T		CIFAR-10, 5T		CIFAR-100, 5T		TinyImagenet, 5T	
	$\bar{A}_T$ ↑	$\bar{F}_T$ ↓	A_T ↑	F_T ↓	A_T ↑	F_T ↓	A_T ↑	F_T ↓
Exemplar-free baselines								
Finetune	27.46 ± 0.89	95.86 ± 1.28	15.89 ± 0.76	78.54 ± 0.87	16.48 ± 2.63	56.65 ± 3.24	13.20 ± 2.23	43.50 ± 0.45
EWC	30.05 ± 0.79	94.13 ± 2.26	18.72 ± 1.92	75.66 ± 3.01	15.79 ± 1.58	55.79 ± 3.87	13.07 ± 3.55	43.04 ± 2.41
SI	29.64 ± 0.35	94.21 ± 1.66	18.96 ± 1.83	74.19 ± 1.48	13.30 ± 2.62	**50.59 ± 3.50**	10.51 ± 3.01	39.19 ± 3.91
LwF	30.16 ± 0.23	94.94 ± 1.33	19.01 ± 0.49	75.00 ± 0.91	**17.92 ± 0.10**	56.85 ± 2.54	13.47 ± 1.48	43.75 ± 1.15
Adam-NSCL	30.23 ± 1.02	94.82 ± 0.53	20.60 ± 0.71	76.82 ± 1.72	17.70 ± 0.85	72.35 ± 1.25	**14.15 ± 2.19**	62.71 ± 2.93
Ours								
IG-CL-freeze-all	**31.55 ± 0.13**	**92.69 ± 0.81**	**21.14 ± 1.90**	**70.68 ± 1.72**	14.66 ± 1.81	51.17 ± 2.48	11.20 ± 0.48	**37.85 ± 0.83**
IG-CL-freeze-part	30.55 ± 0.84	94.47 ± 1.12	20.71 ± 2.29	71.42 ± 2.38	15.17 ± 3.47	52.99 ± 2.85	11.34 ± 3.67	38.53 ± 0.69
Ours Improvement	**+1.32**	+1.44	+0.54	**+3.51**	-2.75	-0.58	-2.81	+1.34
Exemplar-based baselines								
GEM	34.59 ± 0.05	**90.00 ± 3.80**	22.51 ± 0.22	73.50 ± 3.61	19.07 ± 0.62	52.87 ± 2.74	**11.12 ± 1.79**	37.58 ± 1.15
Ours								
IG-CL-freeze-all-GEM	35.60 ± 0.62	94.93 ± 0.66	**24.66 ± 1.63**	**68.96 ± 0.55**	**25.68 ± 1.72**	**36.83 ± 0.26**	9.89 ± 2.56	**33.45 ± 3.05**
IG-CL-freeze-part-GEM	**37.00 ± 0.96**	92.22 ± 2.00	23.22 ± 1.48	72.18 ± 2.73	23.70 ± 3.84	43.73 ± 3.81	10.91 ± 2.26	36.37 ± 2.35
Ours Improvement	**+2.41**	-2.22	**+2.15**	**+4.54**	**+6.61**	**+16.04**	-0.21	**+4.13**
Exemplar-based baselines								
MIR	28.97 ± 2.34	**89.80 ± 0.99**	28.18 ± 1.73	47.71 ± 1.82	9.75 ± 3.39	**43.09 ± 0.68**	10.91 ± 3.89	38.42 ± 1.57
Ours								
IG-CL-freeze-all-MIR	30.23 ± 1.54	91.04 ± 2.57	33.16 ± 3.82	**42.00 ± 2.92**	14.49 ± 0.05	43.82 ± 0.12	12.29 ± 0.60	**38.42 ± 1.78**
IG-CL-freeze-part-MIR	**30.75 ± 1.37**	91.07 ± 2.04	**34.88 ± 1.48**	42.11 ± 2.11	**14.57 ± 2.99**	44.41 ± 1.38	**12.47 ± 1.02**	38.50 ± 3.76
Ours Improvement	+1.78	-1.24	**+6.70**	**+5.71**	**+4.82**	-0.73	+1.56	0.00

Table 11: Accuracy comparison for IN2. All models are pre-trained on the Place365 dataset Zhou et al. (2017). ↑ means larger values are better, while ↓ means smaller values are better. Underline means the strongest baseline, and **boldface** means the best number. In the **Ours Improvement** rows, +/- measures our best number minus the strongest baseline, and the value is in blue if our improvement is statistically significant.

	CIFAR-10, 5T		CIFAR-10, 5T		CIFAR-100, 5T		TinyImagenet, 5T	
	$\bar{A}_T$ ↑	$\bar{F}_T$ ↓	A_T ↑	F_T ↓	A_T ↑	F_T ↓	A_T ↑	F_T ↓
Exemplar-free baselines								
Finetune	29.13 ± 0.28	97.78 ± 0.78	17.99 ± 2.26	79.66 ± 0.72	17.65 ± 2.55	64.94 ± 2.15	15.34 ± 3.83	54.81 ± 0.71
EWC	30.79 ± 0.21	97.92 ± 0.78	19.00 ± 1.87	76.92 ± 0.77	17.44 ± 3.98	64.43 ± 1.84	15.07 ± 2.23	54.77 ± 0.54
SI	30.25 ± 0.72	96.55 ± 1.70	19.31 ± 0.62	74.78 ± 1.55	17.12 ± 3.89	63.11 ± 1.03	14.47 ± 1.02	53.69 ± 1.32
LwF	30.76 ± 0.31	97.75 ± 0.84	19.11 ± 0.44	76.56 ± 1.12	**19.98 ± 0.64**	63.79 ± 2.65	**17.08 ± 1.50**	55.40 ± 1.85
Adam-NSCL	30.78 ± 0.82	96.82 ± 2.35	21.60 ± 0.48	77.73 ± 0.86	16.23 ± 3.39	66.26 ± 3.18	13.44 ± 1.70	58.86 ± 0.70
Ours								
Finetune-CBM	30.39 ± 0.67	93.09 ± 2.22	21.14 ± 0.83	69.47 ± 1.29	16.43 ± 2.82	55.76 ± 3.55	14.91 ± 0.65	51.39 ± 3.78
IN2	**32.25 ± 0.76**	**88.58 ± 0.30**	**22.16 ± 1.73**	**67.92 ± 0.72**	16.37 ± 3.82	**45.71 ± 2.55**	15.68 ± 1.84	**39.40 ± 2.86**
Ours Improvement	**+1.46**	**+7.97**	+0.56	**+6.86**	-3.55	**+17.40**	-1.40	**+14.29**
Exemplar-based baselines								
GEM	36.27 ± 1.86	69.38 ± 2.88	24.11 ± 1.74	**59.84 ± 1.27**	20.67 ± 1.75	63.49 ± 3.15	**5.64 ± 0.38**	37.52 ± 0.02
Ours								
IN2-GEM	**36.37 ± 1.74**	**44.72 ± 2.71**	**28.93 ± 2.09**	61.86 ± 2.73	**23.64 ± 3.82**	**58.54 ± 3.75**	5.37 ± 1.67	**29.06 ± 3.74**
Ours Improvement	+0.10	**+24.66**	**+4.82**	-2.02	**+2.97**	-4.95	-0.27	**+8.46**
Exemplar-based baselines								
MIR	33.20 ± 2.92	75.51 ± 1.94	**33.99 ± 2.00**	48.50 ± 2.32	8.33 ± 0.64	**46.33 ± 2.06**	2.97 ± 3.69	**32.09 ± 0.53**
Ours								
IN2-MIR	**36.61 ± 1.77**	**70.45 ± 1.89**	33.94 ± 1.25	**38.93 ± 1.74**	**13.81 ± 1.94**	54.76 ± 1.59	**5.07 ± 3.66**	34.75 ± 1.54
Ours Improvement	**+3.41**	**+5.06**	-0.05	**+9.57**	**+5.48**	-8.43	+2.10	-2.66

B.4 10, 20 tasks Experiment Results

Table 12 reports comparison for IG-CL under 10-tasks scenario for CIFAR-100 and TinyImagenet. Compared with exemplar-free baselines, IG-CL generally forgets less as F_T and $\bar{F}_T$ shown. However, IG-CL sometimes is worse in A_T and $\bar{A}_T$, which is the limitation of our methods. We view this as the future works to be improved, since this paper's goal is to retain intepretable concepts in models. Nevertheless, IG-CL generally improves exemplar-based baselines when combined with them, which is same as 5-tasks scenario.

Table 13 reports comparison for IN2 under 10-tasks scenario for CIFAR-100 and TinyImagenet. Similar to IG-CL, IN2 performs well in forgetting metrics F_T and $\bar{F}_T$, but performs worse in A_T and $\bar{A}_T$ when comparing with exemplar-free baselines. We believes this is partially because LF-CBM's training procedure is different than standard end-to-end training. As LF-CBM Oikarinen et al. (2023) paper shown, LF-CBM's classification accuracy is usually worse than standard model's. Again, we view this as future works to be improved. Besides, IN2 still can improve exemplar-based baselines when combine with them.

Table 14 and 15 report comparison for IG-CL and IN2 under 20-tasks scenario in CIFAR-100 respectively. Similar to 10-tasks scenario, our methods can improve exemplar-based baselines when combine with them, while the comparison with exemplar-free methods is still under the same trend.

We observe that both of our proposed methods can improve exemplar-based methods when combined with them. When compared with exemplar-free methods, our methods forget less while slightly worse than the strongest baselines in terms of $\bar{A}_T$. Nonetheless, we would like to highlight that our work is the first to bridge continual learning and neuron interpretability with competitive results, which opens up a new and promising direction to transform continual learning from a black-box process to more transparent.

Table 12: Accuracy comparison for IG-CL in 10 tasks scenario. ↑ means larger values are better, while ↓ means smaller values are better. Underline means the strongest baseline, and **boldface** means the best number. In the **Ours Improvement** rows, +/- measures our best number minus the strongest baseline, and the value is in blue if our improvement is statistically significant.

	CIFAR-100, 10T				TinyImagenet, 10T			
	A_T ↑	F_T ↓	$\bar{A}_T$ ↑	$\bar{F}_T$ ↓	A_T ↑	F_T ↓	$\bar{A}_T$ ↑	$\bar{F}_T$ ↓
Exemplar-free baselines								
Finetune	6.49 ± 1.23	65.31 ± 1.32	13.87 ± 0.83	64.20 ± 1.52	5.15 ± 2.13	49.07 ± 0.57	10.23 ± 1.35	45.83 ± 0.21
EWC	6.71 ± 0.63	65.32 ± 1.12	13.88 ± 0.45	63.90 ± 0.94	5.48 ± 2.35	47.42 ± 1.47	10.11 ± 2.12	45.19 ± 1.29
SI	6.74 ± 1.17	66.07 ± 1.91	14.01 ± 1.37	64.39 ± 1.33	5.39 ± 1.57	**44.68 ± 1.40**	10.33 ± 1.32	46.21 ± 1.36
LwF	7.85 ± 2.21	64.13 ± 2.19	**15.02 ± 2.85**	62.66 ± 1.25	5.95 ± 2.35	52.17 ± 1.26	10.82 ± 2.35	45.57 ± 1.36
Adam-NSCL	**7.95 ± 2.77**	62.54 ± 1.89	13.69 ± 2.15	**61.54 ± 2.40**	**6.63 ± 2.23**	49.43 ± 1.45	10.63 ± 1.33	49.43 ± 1.45
Ours								
IG-CL-freeze-all	6.99 ± 1.20	**62.23 ± 0.36**	13.81 ± 1.45	62.79 ± 1.70	5.76 ± 2.67	48.89 ± 2.17	11.24 ± 0.34	49.39 ± 1.92
IG-CL-freeze-part	6.97 ± 1.26	64.03 ± 1.32	13.71 ± 1.36	63.28 ± 1.04	5.86 ± 0.56	49.99 ± 2.16	**11.25 ± 1.28**	**45.00 ± 1.20**
Ours Improvement	-0.96	+0.31	-1.21	-1.74	-0.77	-4.21	+0.43	+0.19
Exemplar-based baselines								
GEM	8.25 ± 1.07	60.31 ± 4.25	15.71 ± 1.35	58.77 ± 2.42	**6.00 ± 2.34**	47.13 ± 1.25	**10.74 ± 2.62**	47.68 ± 1.67
Ours								
IG-CL-freeze-all-GEM	**15.61 ± 1.02**	**52.01 ± 1.34**	**29.83 ± 2.15**	**52.43 ± 2.36**	3.03 ± 3.05	**22.39 ± 3.91**	7.75 ± 2.90	34.75 ± 2.37
IG-CL-freeze-part-GEM	7.65 ± 1.85	60.12 ± 1.37	14.84 ± 1.39	54.12 ± 2.73	2.97 ± 2.34	24.91 ± 2.02	5.52 ± 2.40	**30.44 ± 2.59**
Ours Improvement	**+7.36**	**+8.30**	**+14.12**	**+6.34**	-2.97	**+24.74**	-2.99	**+17.24**
Exemplar-based baselines								
MIR	4.64 ± 0.37	59.37 ± 1.96	12.61 ± 1.02	60.51 ± 1.72	4.54 ± 0.82	46.19 ± 2.43	**10.11 ± 1.34**	46.19 ± 2.17
Ours								
IG-CL-freeze-all-MIR	**5.43 ± 1.54**	**52.22 ± 1.65**	12.86 ± 1.08	**56.19 ± 2.30**	5.09 ± 3.21	**41.34 ± 1.28**	9.97 ± 2.41	**43.21 ± 1.32**
IG-CL-freeze-part-MIR	5.42 ± 1.34	52.34 ± 1.37	**12.89 ± 0.62**	56.72 ± 1.84	**5.17 ± 2.58**	42.87 ± 0.99	9.99 ± 1.23	43.23 ± 1.41
Ours Improvement	+0.79	**+7.15**	+0.28	**+4.32**	+0.63	**+4.85**	-0.12	**+2.98**

Table 13: Accuracy comparison for IN2 in 10 tasks scenario. All models are pre-trained on the Place365 dataset Zhou et al. (2017). ↑ means larger values are better, while ↓ means smaller values are better. Underline means the strongest baseline, and **boldface** means the best number. In the **Ours Improvement** rows, +/- measures our best number minus the strongest baseline, and the value is in blue if our improvement is statistically significant.

	CIFAR-100, 10T				TinyImagenet, 10T			
	$A_T \uparrow$	$F_T \downarrow$	$\bar{A}_T \uparrow$	$\bar{F}_T \downarrow$	$A_T \uparrow$	$F_T \downarrow$	$\bar{A}_T \uparrow$	$\bar{F}_T \downarrow$
Exemplar-free baselines								
Finetune	8.09 ± 1.82	80.43 ± 1.42	17.34 ± 1.87	81.23 ± 2.30	4.61 ± 0.18	66.40 ± 3.42	14.62 ± 0.58	70.70 ± 1.56
EWC	7.59 ± 1.32	80.99 ± 1.28	17.23 ± 0.96	81.08 ± 2.34	5.62 ± 2.38	67.27 ± 1.30	14.88 ± 1.28	71.25 ± 1.38
SI	8.54 ± 1.29	81.43 ± 1.83	17.53 ± 0.65	81.60 ± 2.45	7.90 ± 1.40	71.59 ± 0.82	15.65 ± 1.19	72.33 ± 2.08
LwF	13.83 ± 1.26	77.21 ± 1.53	**24.99 ± 2.29**	71.19 ± 3.33	**10.40 ± 2.35**	71.40 ± 1.59	**20.42 ± 1.86**	66.78 ± 3.95
Adam-NSCL	**14.29 ± 1.19**	69.75 ± 3.15	23.19 ± 1.38	76.24 ± 1.29	9.74 ± 2.23	66.87 ± 1.45	18.63 ± 2.45	69.97 ± 1.24
Ours								
Finetune-CBM	7.31 ± 0.82	68.88 ± 1.40	14.91 ± 1.28	66.72 ± 2.73	7.18 ± 1.26	65.76 ± 1.42	14.41 ± 1.89	64.64 ± 3.02
IN2	7.34 ± 1.68	**37.90 ± 1.59**	14.98 ± 1.09	**61.96 ± 1.73**	7.37 ± 2.54	**56.80 ± 1.27**	14.98 ± 2.93	**60.02 ± 3.09**
Ours Improvement	-6.95	**+31.85**	-10.01	**+9.23**	-3.03	**+9.60**	-5.44	**+6.76**
Exemplar-based baselines								
GEM	**11.47 ± 1.32**	66.44 ± 3.14	22.21 ± 1.20	70.54 ± 2.32	4.12 ± 1.79	54.29 ± 1.62	13.44 ± 1.33	63.58 ± 1.11
Ours								
IN2-GEM	8.68 ± 2.41	**53.13 ± 3.71**	**22.46 ± 1.15**	**59.36 ± 2.33**	**6.20 ± 3.07**	**47.95 ± 1.48**	**14.96 ± 3.48**	**57.94 ± 1.26**
Ours Improvement	-2.79	**+13.31**	+0.25	**+11.18**	+2.08	**+6.34**	+1.52	**+5.64**
Exemplar-based baselines								
MIR	3.24 ± 2.09	**58.77 ± 1.69**	14.19 ± 2.21	73.32 ± 0.93	3.37 ± 0.84	**58.83 ± 2.06**	9.40 ± 3.29	**59.29 ± 4.20**
Ours								
IN2-MIR	**8.38 ± 1.35**	71.02 ± 2.06	**16.65 ± 2.23**	**70.49 ± 1.90**	**7.13 ± 2.15**	60.98 ± 2.38	**14.07 ± 2.31**	61.14 ± 2.36
Ours Improvement	**+5.14**	**+12.25**	**+2.46**	**+2.83**	**+3.76**	-2.15	**+4.67**	-1.85

Table 14: Accuracy comparison for IG-CL in 20 tasks scenario. ↑ means larger values are better, while ↓ means smaller values are better. Underline means the strongest baseline, and **boldface** means the best number. In the **Ours Improvement** rows, +/- measures our best number minus the strongest baseline, and the value is in blue if our improvement is statistically significant.

	CIFAR-100, 20T			
	$A_T \uparrow$	$F_T \downarrow$	$\bar{A}_T \uparrow$	$\bar{F}_T \downarrow$
Exemplar-free baselines				
Finetune	3.80 ± 2.26	69.05 ± 2.23	9.72 ± 3.54	70.25 ± 0.88
EWC	3.56 ± 0.16	68.67 ± 0.71	9.72 ± 2.72	70.11 ± 3.29
SI	3.92 ± 2.37	76.58 ± 3.77	10.61 ± 1.65	76.19 ± 0.00
LwF	4.14 ± 2.12	77.06 ± 1.48	10.54 ± 3.72	75.25 ± 2.74
Adam-NSCL	**10.59 ± 0.99**	67.32 ± 3.52	**19.45 ± 2.85**	68.21 ± 2.80
Ours				
IG-CL-freeze-all	3.35 ± 1.13	**63.12 ± 3.02**	8.82 ± 2.43	**65.21 ± 2.34**
IG-CL-freeze-part	3.79 ± 2.52	72.40 ± 3.61	9.99 ± 2.24	72.52 ± 1.42
Ours Improvement	-6.80	**+4.20**	-9.46	**+3.00**
Exemplar-based baselines				
GEM	14.90 ± 3.79	70.56 ± 3.06	24.88 ± 3.34	66.55 ± 0.44
Ours				
IG-CL-freeze-all-GEM	**20.72 ± 0.88**	**35.48 ± 2.14**	**27.73 ± 2.84**	**66.51 ± 1.72**
IG-CL-freeze-part-GEM	17.40 ± 3.74	63.10 ± 2.51	24.18 ± 2.34	68.03 ± 2.30
Ours Improvement	**+5.82**	**+35.08**	**+2.85**	+0.04
Exemplar-based baselines				
MIR	11.32 ± 2.07	45.31 ± 0.08	17.49 ± 3.68	57.71 ± 2.67
Ours				
IG-CL-freeze-all-MIR	12.75 ± 0.68	**39.36 ± 2.46**	17.17 ± 2.60	**41.74 ± 0.31**
IG-CL-freeze-part-MIR	**13.03 ± 1.71**	52.47 ± 0.30	**18.02 ± 3.30**	53.93 ± 3.61
Ours Improvement	+1.71	**+5.95**	+0.53	**+15.97**

Table 15: Accuracy comparison for IN2 in 20 tasks scenario. All models are pre-trained on the Place365 dataset Zhou et al. (2017). ↑ means larger values are better, while ↓ means smaller values are better. Underline means the strongest baseline, and **boldface** means the best number. In the **Ours Improvement** rows, +/- measures our best number minus the strongest baseline, and the value is in blue if our improvement is statistically significant.

	CIFAR-100, 20T			
	$A_T \uparrow$	$F_T \downarrow$	$\bar{A}_T \uparrow$	$\bar{F}_T \downarrow$
Exemplar-free baselines				
Finetune	4.03 ± 0.60	71.17 ± 0.86	10.35 ± 1.38	77.07 ± 3.09
EWC	3.92 ± 3.23	73.90 ± 2.41	10.65 ± 1.20	78.75 ± 3.67
SI	3.73 ± 0.45	78.96 ± 0.36	11.21 ± 2.85	82.57 ± 3.67
LwF	5.23 ± 3.18	85.31 ± 2.62	13.32 ± 3.94	85.45 ± 3.49
Adam-NSCL	**10.93 ± 1.33**	69.52 ± 0.54	**17.96 ± 0.74**	87.83 ± 2.50
Ours				
Finetune-CBM	4.05 ± 3.87	77.40 ± 3.48	10.67 ± 0.05	74.86 ± 3.00
IN2	4.04 ± 2.87	**66.55 ± 3.23**	11.48 ± 1.18	**73.06 ± 0.29**
Ours Improvement	-6.88	**+2.97**	-6.48	**+4.01**
Exemplar-based baselines				
GEM	12.59 ± 2.84	**58.33 ± 2.69**	22.94 ± 0.34	**67.12 ± 2.08**
Ours				
IN2-GEM	**12.87 ± 2.37**	61.74 ± 3.69	**25.62 ± 2.83**	68.64 ± 0.53
Improvement	+0.28	-3.41	**+2.68**	-1.52
Exemplar-based baselines				
MIR	11.01 ± 1.01	**29.39 ± 2.81**	16.68 ± 0.41	**51.33 ± 1.35**
Ours				
IN2-MIR	**12.53 ± 0.08**	36.31 ± 1.58	**19.55 ± 1.90**	55.79 ± 1.79
Ours Improvement	**+1.52**	-6.92	**+2.87**	-4.46

B.5 Comparison with More baselines

In this section, we do individual comparisons with SSRE (Zhu et al., 2022), DEN (Yoon et al., 2017) and ICICLE (Rymarczyk et al., 2023).

B.5.1 Comparison with SSRE

We compare our methods with SSRE (Zhu et al., 2022). Since we can not access the pre-training details described in SSRE paper, we compare our IG-CL with SSRE that is trained from scratch. Besides metrics described in Section 5.1, we also measure **Learning Accuracy** ($F_T = \frac{1}{T}\sum_{i=1}^{T} a_{i,i}$) (Mirzadeh et al., 2022b; Riemer et al., 2018; Yin et al., 2021; Mirzadeh et al., 2022a) to understand model's ability to learn new tasks. Experiment results are in Table 16. IG-CL forgets more as the performace in F_T is worse. However, it has much better learning ability as L_T shown.

Table 16: Comparison between IG-CL and SSRE Zhu et al. (2022) in CIFAR-10 and CIFAR-100. ↑ means larger values are better, while ↓ means smaller values are better. Even though IG-CL forgets more, it has better learning ability.

	CIFAR-10, 5T			CIFAR-100, 5T			CIFAR-100, 10T			CIFAR-100, 20T			TinyImagenet, 5T			TinyImagenet, 10T		
	$A_T \uparrow$	$F_T \downarrow$	$L_T \uparrow$	$A_T \uparrow$	$F_T \downarrow$	$L_T \uparrow$	$A_T \uparrow$	$F_T \downarrow$	$L_T \uparrow$	$A_T \uparrow$	$F_T \downarrow$	$L_T \uparrow$	$A_T \uparrow$	$F_T \downarrow$	$L_T \uparrow$	$A_T \uparrow$	$F_T \downarrow$	$L_T \uparrow$
SSRE	**28.44**	**15.96**	36.18	**31.55**	**7.97**	32.73	**17.72**	**7.46**	11.29	**8.94**	**6.73**	4.51	**13.76**	**6.06**	13.59	**11.44**	**7.33**	15.83
IG-CL-freezed-all	21.14	70.68	**93.29**	16.66	51.17	**63.22**	6.99	62.23	**64.25**	3.35	63.12	**66.46**	13.20	37.85	**47.92**	5.76	48.89	**49.81**

B.5.2 Comparison with DEN

We compare our methods with DEN (Yoon et al., 2017) in the CIFAR-10 and CIFAR-100 dataset. We combine a pretrained model with a 2-layer DEN, and compare it with Finetune-CBM and IN2. The experiment results are in Table 17. IN2 and Finetune-CBM outperform DEN by up to 20.01% and 18.15% in $\bar{A}_T$ respectively.

B.5.3 Comparison with ICICLE

We compare IN2 with ICICLE (Rymarczyk et al., 2023) in the CUB200 (Wah et al., 2011) dataset. CUB200 is a bird species classification dataset that has 200 classes with 5994 training examples and 5794 testing examples. The experiment results are in Table 18. Our method outperforms ICICLE by 2.02% in $\bar{A}_T$ and 31.68% in $\bar{F}_T$.

Table 17: Comparison between DEN (Yoon et al., 2017) and our methods, in the 5-task scenario of CIFAR-10 and CIFAR-100. The experiment results shows that our methods outperform DEN in $\bar{A}_T$ by large margins.

	CIFAR-10, 5T		CIFAR-100, 5T	
	$\bar{A}_T \uparrow$	$\bar{F}_T \downarrow$	$\bar{A}_T \uparrow$	$\bar{F}_T \downarrow$
DEN	12.24	**19.20**	9.18	**10.50**
Finetune-CBM (Ours)	30.39	93.09	**24.99**	59.29
IN2 (Ours)	**32.25**	88.58	24.25	47.62

Table 18: Comparison between IN2 and ICICLE (Rymarczyk et al., 2023) and other baselines in CUB200 5-task scenario. IN2 outperform ICICLE in both $\bar{A}_T$ and $\bar{F}_T$.

	CUB200, 5T	
	$\bar{A}_T \uparrow$	$\bar{F}_T \downarrow$
Exemplar-free baselines		
Finetune	10.16	60.73
EWC	11.02	62.43
LwF	12.50	64.50
Adam-NSCL	<u>13.27</u>	<u>40.73</u>
ICICLE	11.40	53.66
Ours		
IN2	**13.42**	**21.98**

B.6 Forward Transfer Metric

We use Forward Transfer Metric (FWT) Lopez-Paz & Ranzato (2017) to measure our methods' ability to reuse old knowledge on new tasks. We did experiments on CUB200, 5 tasks scenario since CUB200 shares several concepts among classes. Table 19 and 20 show that our methods have better abilities to share knowledge from old tasks to new tasks compared with baselines.

Table 19: Forward Transfer (FWT) Metric comparison for IG-CL. Our methods outperform the baselines on FWT by large margins.

	CUB200, 5T
	$FWT \uparrow$
Exemplar-free baselines	
Finetune	0.76
EWC	3.83
SI	13.50
LwF	10.20
Adam-NSCL	21.04
Ours	
IG-CL-freeze-all	28.79
IG-CL-freeze-part	**30.07**
Exemplar-based baselines	
GEM	1.35
Ours	
IG-CL-freeze-all-GEM	**26.76**
IG-CL-freeze-part-GEM	26.68
Exemplar-based baselines	
MIR	-12.44
Ours	
IG-CL-freeze-all-MIR	6.89
IG-CL-freeze-part-MIR	**8.22**

Table 20: Forward Transfer (FWT) Metric comparison for IN2. Our methods outperform the baselines on FWT by large margins.

	CUB200, 5T
	$FWT \uparrow$
Exemplar-free baselines	
Finetune	1.43
EWC	6.88
SI	11.67
LwF	10.36
Adam-NSCL	**17.63**
Ours	
Finetune-CBM	16.71
IN2	12.66
Exemplar-based baselines	
GEM	19.98
Ours	
IN2-GEM	**27.78**
Exemplar-based baselines	
MIR	3.20
Ours	
IG-CL-freeze-all-MIR	**9.84**

B.7 Experiment results on ImageNet-10

We conduct experiments on large scale dataset ImageNet-10, and the results are in Table 21 and 22. The experiment results are still under the same trend as other datasets: Our methods outperform other exemplar-free methods by up to 0.87% in $\bar{A}_T$ and up to 5.77% in $\bar{F}_T$. Meanwhile, can improve exemplar-based methods by combining them by up to 1.83% in $\bar{A}_T$ and up to 2.87% in $\bar{F}_T$

Table 21: Experiment results on ImageNet-10 in the 5-task scenario.

	$\bar{A}_T \uparrow$	$\bar{F}_T \downarrow$
Finetune	23.33 ± 0.75	81.20 ± 1.10
EWC	24.14 ± 0.69	78.46 ± 1.32
IG-CL-freeze-all (Ours)	**25.01** ± 0.51	**77.20** ± 0.95
GEM	31.34 ± 0.82	61.71 ± 0.82
IG-CL-freeze-all-GEM (Ours)	**33.17** ± 0.50	**59.65** ± 1.29

Table 22: Experiment results on ImageNet-10 in the 5-task scenario, the backbones are pretrained on Place365 dataset.

	$\bar{A}_T \uparrow$	$\bar{F}_T \downarrow$
Finetune	23.83 ± 0.93	81.92 ± 1.38
EWC	25.40 ± 0.39	78.98 ± 1.51
IN2 (Ours)	**26.12** ± 0.84	**73.21** ± 1.73
GEM	32.66 ± 0.85	60.27 ± 1.32
IN2-GEM (Ours)	**34.37** ± 0.43	**57.40** ± 0.99

B.8 Impact from the order of tasks

To understand the impact from the order of tasks, we conducted experiments on CIFAR-100 using the class distribution outlined in Table 39, where similar classes are grouped into the same task. We then swapped the order of task 1 and task 2 and compared the results with the original task order. The continual learning performance for IG-CL is in Table 23, and IN2 is in Table 24. In both task orders, our methods consistently preserve learned knowledge effectively. IG-CL and IN2 outperform other exemplar-free methods by up to 0.14% in $\bar{A}_T$ and up to 26.39% in $\bar{F}_T$. Additionally, they improve upon exemplar-based methods by up to 1.45% in $\bar{A}_T$ and up to 11% in $\bar{F}_T$. These results demonstrate that our methods are robust to changes in task order.

We also analyze the concept evolution of two methods like Section 5.3. For IG-CL, the concept evolution analysis is in Table 25. Same as the original order that analyzed in Table 4, IG-CL can preserve concepts even after learning a unrelated task. For IN2, the analysis is in Figure 9. Same as the original order that analyzed in Figure 5, IN2 can preserve concepts while finetune CBM loss all of the significant weights. Overall, the concept evolution analysis show that our methods can preserved learned concepts regardless of the task order.

Table 23: Continual learning performance on CIFAR-100 5-task scenario. Original order is the class distribution in Table 39, and Swap order exchanges the task 1 and task 2 of it. IG-CL has better $\bar{F}_T$ and similar or better $\bar{A}_T$.

	Original order		Swap order	
	$\bar{A}_T \uparrow$	$\bar{F}_T \downarrow$	$\bar{A}_T \uparrow$	$\bar{F}_T \downarrow$
Naive	12.83	45.01	12.50	47.94
SI	13.10	41.10	12.87	47.03
LwF	14.47	41.83	**14.36**	47.00
IG-CL-freeze-all	13.93	**36.85**	13.63	**43.36**
IG-CL-freeze-part	**14.61**	39.19	13.33	46.29
GEM	16.57	40.31	16.01	45.92
IG-CL-freeze-all-GEM	**17.23**	**29.31**	**16.43**	**40.41**
IG-CL-freeze-part-GEM	15.88	34.54	15.08	41.91

Table 24: Continual learning performance on CIFAR-100 5-task scenario. Original order is the class distribution in Table 39, and Swap order exchanges the task 1 and task 2 of it. IN2 has better $\bar{F}_T$ and similar or better $\bar{A}_T$.

	Original order		Swap order	
	$\bar{A}_T \uparrow$	$\bar{F}_T \downarrow$	$\bar{A}_T \uparrow$	$\bar{F}_T \downarrow$
Naive	14.64	56.16	14.27	59.95
SI	15.20	55.98	15.58	59.12
LwF	**18.32**	55.26	**18.74**	52.13
finetune_cbm	13.95	37.51	11.41	42.29
IN2	15.34	**28.87**	16.23	**33.32**
GEM	17.02	55.35	20.61	53.22
IN2-GEM	**18.15**	**48.50**	**22.06**	**52.71**

Table 25: Concept evolution for IG-CL in freeze-all implementation, testing on class distribution 39 but swap task 1 and task 2. We analyse the concept evolution in the layer 4 of ResNet18. The blue concept means the concept is related to the current task, while the green concept means it is unrelated. "x" stands for non-interpretable units. The results show that IG-CL can preserve the concepts from previous classes.

CIFAR-100, 5T					
	task 1	task 2	task 3	task 4	task 5
Classes	Natural scenes & Plants	Small animals & Sea animals	Big animals	Big objects	Others
Unit 275	landscapes	landscapes	landscapes	x	x
Unit 140	x	x	zebra	zebra	x

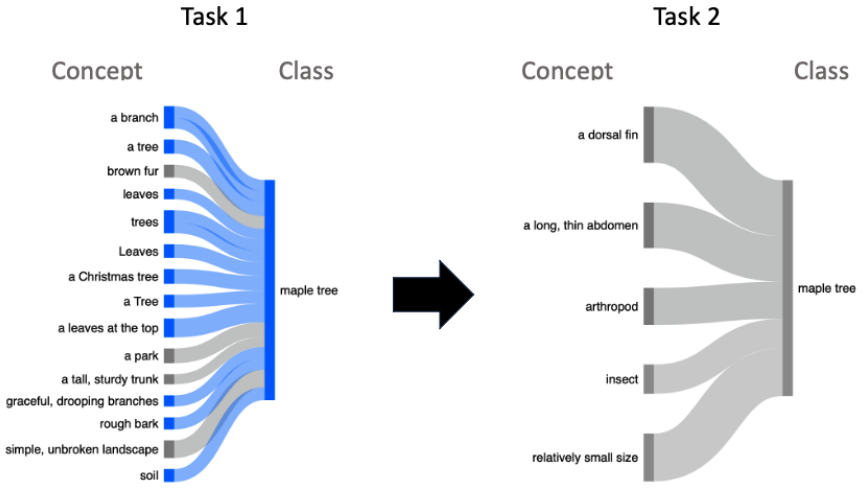

(a) Finetune-CBM

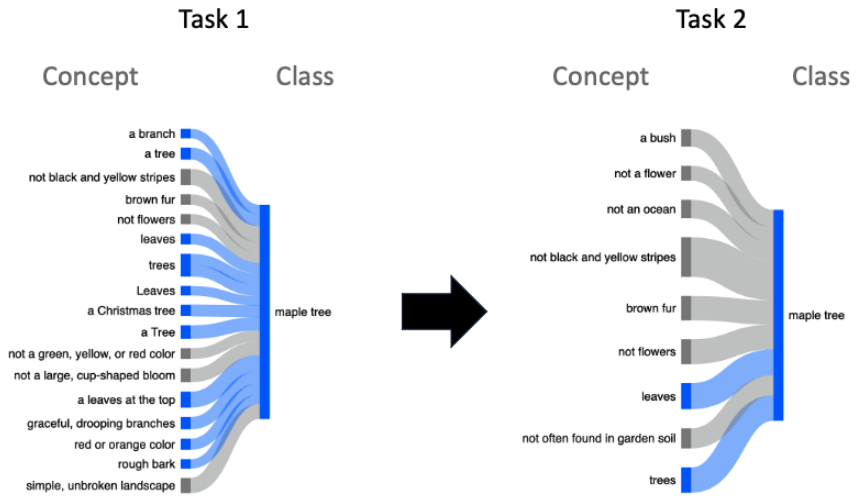

(b) IN2

Figure 9: Final weight visualization for random classes in (a) Finetune-CBM and (b) IN2 trained on CIFAR-100 under 5-tasks scenario. The class distribution is in Table 39 but swap task 1 and task 2. For class "maple tree" from task 1, we show its significant weight (> 0.16) after training on task 1 and task 2. Concepts generated from the maple tree class itself are colored blue, and other concepts from task 1 are colored gray. We can see IN2 keeps a similar final layer while Finetune-CBM loses most significant weights.

C Further Analysis and Details

C.1 Computational efficiency

Table 26 shows the maximum GPU usage of Finetune, EWC, GEM and our methods on CIFAR-10 under 5-tasks scenario. Even integrated with the interpretable tool CLIP-Dissect (Oikarinen & Weng, 2022), IG-CL's maximum GPU usage is still lower than EWC and GEM. Meanwhile, IN2's memory usage is efficient even though the CBL layer increases when learning new tasks. The experiment results show our methods are efficient.

Table 26: Maximum GPU usage comparison for our methods, under CIFAR-10 5-tasks scenario. IG-CL's maximum GPU usage is smaller than EWC and GEM, which shows IG-CL's computational efficiency. IN2 is more efficient than existing methods.

Method	Finetune	EWC	GEM	IG-CL-freeze-all/ IG-CL-freeze-part	IN2
Max GPU usage (GB)	5.51	5.65	5.68	5.61	4.00

C.2 Interpretability Guided Continual Learning Algorithm

The algorithm 1 summarizes the procedure of **Interpretability Guided Continual Learning**.

Algorithm 1 IG-CL: Freeze the subnetworks of the concept units

Require: Dataset $\mathbb{D}$; regularization coefficient μ; connection threshold τ; regularization factor λ; Neural network parameters $\boldsymbol{\theta}$

for $t \leftarrow$1,...,T **do**
  if t is 1 **then**
    Train $\boldsymbol{\theta^1}$ on D_t by solving $\min_{\boldsymbol{\theta}^1} \mathcal{L}(\boldsymbol{\theta}^1; \mathcal{D}_1) + \mu \sum_{l=1}^{L} \|\mathbf{W}_l^1\|_{2,1}$
  else
    Train $\boldsymbol{\theta^t}$ on D_t by solving Eq. 1
  `ConceptUnit` $\leftarrow$ CLIP-Dissect(W^t)
  `Prev-active` $\leftarrow$ `ConceptUnit`
  for layer $l \leftarrow$ L,...,1 **do** ▷ Find the subnetwork of the concept units
    for Unit $u_l \leftarrow$ 1,...,U_l **do**
      if `Prev-active`$[u_l]$ is **True then** ▷ u_l is in subnetwork
        for Unit $u_{l-1} \leftarrow$1,...,U_{l-1} **do**
          if $\|\mathbf{W}^t_{u_l,u_{l-1}}\|_1 > \tau$ **then** ▷ weight exceeds threshold
            `Active`$[u_{l-1}] \leftarrow$ **True**
    if Using freeze-all **then**
      $\forall$ `Prev-active`$[u_l]$ is **True**, Freeze $\mathbf{W}^t_{u_l,:}$
      $\forall$ `Active`$[u_{l-1}]$ is **True**, Freeze $\mathbf{W}^t_{:,u_{l-1}}$
    else if Using freeze-part **then**
      $\forall$ `Prev-active`$[u_l]$ is **True**, Freeze $\mathbf{W}^t_{u_l,:}$
    `Prev-active` $\leftarrow$ `Active`

C.3 Details of IG-CL and IN2

In this section, we study the technical details of the IG-CL and IN2. ImageNet-10 is the 10-class subset of ImageNet (Russakovsky et al., 2015). For IG-CL, Figure 10 shows the subnetwork sizes in different datasets. Generally, a more complicated dataset has a bigger subnetwork, but the size is adjustable by tuning hyperparameters.

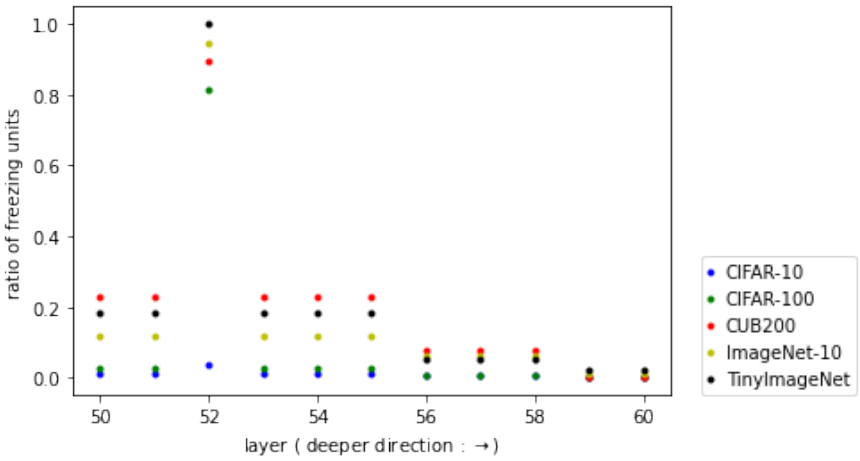

Figure 10: The subnetwork sizes in the last residual block after learning two tasks in the 5-task scenario. A more complicated dataset will have bigger subnetworks.

For IN2, Table 29 and 30 show the number of concepts added per tasks. Overall, larger and more complicated datasets have more concepts. Around 10% of concepts are the same during the concept set expansion 4.2. Table 27 shows some example concepts that are related to different classes. Table 28 shows some complex concepts in IN2 from different datasets.

Concept	Related Classes
ship	vessel, cargo ship
a leaf	apple, rose
a small body	baby, fish
animal	wolf, fish, beetle
vehicle	bicycle, train, streetcar

Table 27: Some concepts that generated from the different classes in IN2.

Dataset	Complex concepts
CIFAR-10	a flatbed for carrying cargo; four round, black tires; long hind legs for jumping
CIFAR-100	a tractor trailer; a soft, round head; a crew of astronauts
TinyImageNet	a second hand or digital timer; a seat that is low to the ground; a double-reed mouthpiece

Table 28: Some complex concepts that generated from the different datasets in IN2.

We build IN2 based on LF-CBM Oikarinen et al. (2023). Therefore, we would like to discuss two properties related to LF-CBM. First, following LF-CBM's procedure, we use CLIP to calculate the activation matrix P as described in Section 2.2. We can replace CLIP with other vision language aligned (VL-aligned) models as long as they have a text encoder and an image encoder to calculate matrix P. One future work will be replacing CLIP with other suitable VL-aligned models.

Second, using GPT-3 to general concept sets is firstly proposed from an earlier work LF-CBM, which has many concurrent and follow-up works that use language models to create concept bottleneck layers (Yang et al., 2023b; Yan et al., 2023). Introducing additional information is widely exploited when designing CBM (Yuksekgonul et al., 2022; Zhou et al., 2018; Losch et al., 2019), and is reasonable task-relevant information that we can leverage. Meanwhile, using additional information to enhance a model's performance is common in other fields as well (Hu et al., 2021; Yang et al., 2023a). Even though LF-CBM has a potential leakage problem when using addtional text information, our method is still under the setting of continual learning. This is because during the training phase, the information for each class only appears in one task. One future work is to handle the potential leaking of CBM.

Table 29: Average concepts added per task in the 5-task scenario.

	CIFAR-10	CIFAR-100	CUB200	ImageNet-10	TinyImageNet
Number of Concept	37.4	133.1	276.6	35.6	301.8

Table 30: Average concepts added per task in the 10-task scenario.

	CIFAR-100	TinyImageNet
Number of Concept	154.6	284.3

D Others

D.1 Experiment Setup and Details

D.1.1 Training and computing details

All models are trained on single NVIDIA V100s (32 GB SMX2). The hyperparameters used for our methods are in Table 31. We tune the hyperparameters for best performance in $\bar{A}_T$. The hyperparameters tuning results are in Table 32, 33, 34 and 35. The hyperparameter selection of λ in Eq. (3) is discussed in Appendix B.2. The tuning process ensures that our methods are fairly compared to other baselines by optimizing their performance under the same conditions. When combine IG-CL or IN2 with GEM (Lopez-Paz & Ranzato, 2017) or MIR (Aljundi et al., 2019), we use the memory buffer size: 150 samples per task. Meanwhile, we experiment GEM and MIR with the same memory buffer size for fair comparisons. We split each dataset by 3 different random seeds, and run each class distribution for 3 times. The code and full training details will be released to public upon acceptance.

Table 31: Hyperparameters for our methods.

μ in Eq. (1)	10^{-6}
λ in Eq. (1)	0.4
λ in Eq. (3)	0
γ in Eq. (3)	0.4
τ in IG-CL's Step 2	0.15

D.1.2 Dataset details and result report

CIFAR-10/ CIFAR-100 and TinyImageNet are standard image classification benchmarks. Both CIFAR-10 and CIFAR-100 have 50k training examples and 10000 testing examples with 10 classes and 100 classes respectively. TinyImageNet has 200 classes with 500 training examples and 50 testing examples per class.

Table 32: IG-CL's performance in different μ of Eq. (1) under CIFAR-100 5-task scenario. The λ of Eq. (1) is set to 0.4 and connection threshold τ is set to 0.15 during the experiments.

	$\bar{A}_T$
$\mu = 10^{-5}$	20.65
$\mu = 10^{-6}$	22.37
$\mu = 10^{-7}$	20.19

Table 33: IG-CL's performance in different λ of Eq. (1) under CIFAR-100 5-task scenario.. The μ of Eq. (1) is set to 10^{-6} and connection threshold τ is set to 0.15 during the experiments.

	$\bar{A}_T$
$\lambda = 0.1$	19.28
$\lambda = 0.4$	22.37
$\lambda = 4$	17.17

Table 34: IN2's performance in different γ of Eq. (3) under CIFAR-100 5-task scenario. The λ of Eq. (1) is set to 0.4 and connection threshold τ is set to 0.15 during the experiments.

	$\bar{A}_T$
$\gamma = 0.1$	22.91
$\gamma = 0.4$	24.99
$\gamma = 4$	18.26

Table 35: IG-CL's performance in different connection threshold τ under CIFAR-100 5-task scenario.. The μ and λ of Eq. (1) is set to 10^{-6} and 0.4 respectively during the experiments.

	$\bar{A}_T$
$\tau = 0.125$	19.24
$\tau = 0.15$	22.37
$\tau = 0.2$	17.61

In experiment results, we perform the independent t-test. We calculate the p-value with confidence interval 95% when comparing our best performance and the strongest baseline. The improvement is mark in blue if the p-value is less than 0.05.

D.2 Extended Previous Works Introduction

In the following sections, we provide detailed introductions to previous continual learning methods, and the details of interpretability tools and models.

D.2.1 Previous Continual Learning Methods

The representative method in regularization-based methods category **(i)** is **Elastic Weight Consolidation (Kirkpatrick et al., 2017)**. Elastic Weight Consolidation (EWC) is a regularized-based method. The loss function in this strategy $L(\boldsymbol{\theta}^t) = L_{\text{CE}}(\boldsymbol{\theta}^t) + \frac{\lambda}{2}\sum_i F_i^t(\theta_i^t - \theta_i^{t-1})^2$ has a quadratic penalty term which is related to the difference between the parameters of the old task and the new task. Meanwhile, this penalty term is proportional to the diagonal of the Fisher information matrix F. λ is a hyperparameter, and $\boldsymbol{\theta}^t, \boldsymbol{\theta}^{t-1}$ stand for model parameters before and after training on a new task t respectively. Similarly, Zenke et al. (2017) adds a quadratic penalty term in the loss function, while estimating the importance of parameters during training. Li & Hoiem (2017) trains models with a knowledge distillation loss for old tasks and a regularization loss to outperform joint training.

The classic method in architecture-based methods category **(ii)** is **Adam-NSCL (Wang et al., 2021)**. For each task, it learns model parameters in the null space of all previous tasks, which is based on Adam. The approximate null space is obtained by using singular value decomposition to the uncentered covariance matrix of input representations of all previous tasks. Yoon et al. (2017) expands and prunes the neural network's architecture when learning new tasks.

The classic method in replay-based methods category **(iii)** is **Gradient Episodic Memory (Lopez-Paz & Ranzato, 2017)**. Gradient Episodic Memory (GEM) is a replay-based method. It stores a subset of the

observed examples from previous tasks, which is described as episodic memory. When training on new tasks, it regularizes the projection of the estimated gradient descent g on the gradient descent of episodic memory g_k. The optimization goal is formalized as $\langle g, g_k \rangle \geq 0, \forall k < t$ when training on the task t. This regularization prevents the loss of episodic memory from increasing. (Rebuffi et al., 2017) stores a subset of samples for each class and uses the nearest-mean classifier on the data representation space.

D.2.2 Detailed introduction to interpretability tools and models

CLIP-Dissect (Oikarinen & Weng, 2022) use the Contrastive Language-Image Pre-training (CLIP) model (Radford et al., 2021) to decipher the neurons in target model. CLIP is composed of an image encoder E_I and a text encoder E_T. Given a probing dataset $\mathcal{D}_{probe} = \{x_i\}_{i=1}^N, x_i \in \mathbb{R}^d$, and a set of concepts $\{c\}_{j=1}^M$, the first step is to generate the representation by the encoders. The results are $\mathbf{I}_i = E_I(x_i), \mathbf{I}_i \in R^{I_0}$ and $\mathbf{C}_j = E_T(c_j), \mathbf{C}_j \in R^{T_0}$. Next, they compute concept-activation matrix $P \in \mathbb{R}^{N \times M}$ where $P_{i,j} = \mathbf{I}_i \cdot \mathbf{C}_j \in \mathbb{R}$. Third, neuron k's activation map is defined as $A_k(x_i)$ for input image x_i. The mean of activation map is described as $g(A_k(x_i)) \in \mathbb{R}$ and the activation vector is $\mathbf{q}_k = [g(A_k(x_1)), ..., g(A_k(x_N))]^T \in \mathbb{R}^N$. Finally, the concept label of neuron k is c_n where n is calculated from the Eq. (4)

$$n = \text{argmax}_m \texttt{sim}(c_m, \mathbf{q}_k; P) \tag{4}$$

where `sim` is similarity function.

Label-Free Concept Bottleneck Model (LF-CBM) (Oikarinen et al., 2023) transforms neural networks into an interpretable CBM without labeled concept data. The procedure in LF-CBM is as follows: First, it uses GPT-3 (Brown et al., 2020) to generate a set C of text concepts important for the task based on class labels, which is then filtered to improve quality. Second, LF-CBM learns a CBL where each neuron corresponds to one of these concepts, by aligning the neurons with CLIP's(Radford et al., 2021) representation of the concepts. Given M concepts generated from the previous step, the CBL is a linear transformation of the pretrained NN backbone $f(x)$, expressed as $W_c \in d_0 \times |C|$. Here d_0 is the output dimension of $f(x)$. W_c is learned to maximize the similarity between CBL's output $f_c(x) = W_c f(x)$ and CLIP's activation matrix P. This incentivizes the k-th neuron to have an activation pattern similar to CLIP with the k-th concept. We denote k-th neuron's, activation pattern as $q_k^\top = [f_{c,k}(x_1), ..., f_{c,k}(x_N)]^\top$. W_c is then optimized by minimizing the following objective: $\sum_{i=1}^M -\frac{\bar{q}_i^3 \cdot \bar{P}_{:,i}^3}{\|\bar{q}_i^3\|_2 \|\bar{P}_{:,i}^3\|_2}$ where $\bar{q}$ means the vector is normalized to have mean 0 and standard derivation 1. Finally, LF-CBM learns a sparse linear prediction layer with weight W_F and bias b_F. The optimization goal is in Eq. (5):

$$\min_{W_f^t, b_f^t} \|W_F f_c(\mathbf{X}_{\text{train}}) + b_F - y\|_2^2 + \lambda R_\alpha(W_F) \tag{5}$$

where $R_\alpha = 0.5(1-\alpha)\|W_F\|_2^2 + \alpha\|W_F\|_1$.

D.3 Class Distribution

Table 36: Classes distribution of CIFAR-10 separated by random seed 3456.

Task 1	automobile, dog
Task 2	deer, horse
Task 3	bird, frog
Task 4	ship, truck
Task 5	airplane, cat

Table 37: Classes distribution of CIFAR-100 separated by random seed 3456.

Task 1	bear, bee, butterfly, camel, caterpillar, chair, elephant, forest, hamster, lion, motorcycle, otter, plates, sea, shark, shrew, spider, tank, train, willow
Task 2	beaver, bowls, boy, bridge, castle, cockroach, couch, dinosaur, house, keyboard, lawn mower, mushrooms, pears, pickup truck, poppies, possum, ray, skyscraper, wardrobe, whale
Task 3	beetle, cloud, crocodile, lamp, leopard, lizard, palm, pine, porcupine, snail, streetcar, sweet peppers, table, telephone, television, tiger, tulips, turtle, woman, worm
Task 4	baby, bed, bicycle, bottles, cans, chimpanzee, crab, lobster, man, maple, mouse, oak, orchids, plain, road, rocket, roses, skunk, squirrel, trout
Task 5	apples, aquarium fish, bus, cattle, clock, cups, dolphin, flatfish, fox, girl, kangaroo, mountain, oranges, rabbit, raccoon, seal, snake, sunflowers, tractor, wolf

Table 38: Classes distribution of CIFAR-100 separated by random seed 5678.

Task 1	bowls, butterfly, cans, cloud, crab, girl, keyboard, leopard, lizard, mountain, mushrooms, pickup truck, roses, seal, snail, spider, squirrel, sunflowers, train, trout
Task 2	baby, bear, bridge, cattle, chimpanzee, cockroach, couch, crocodile, flatfish, lamp, lobster, orchids, palm, plates, sea, shark, shrew, skyscraper, tulips, whale
Task 3	apples, bed, bicycle, bus, caterpillar, cups, elephant, fox, hamster, kangaroo, lawn mower, maple, oak, plain, porcupine, rabbit, road, sweet peppers, tiger, wolf
Task 4	bee, bottles, boy, chair, dinosaur, house, oranges, otter, pine, poppies, ray, snake, tank, telephone, tractor, turtle, wardrobe, willow, woman, worm
Task 5	aquarium fish, beaver, beetle, camel, castle, clock, dolphin, forest, lion, man, motorcycle, mouse, pears, possum, raccoon, rocket, skunk, streetcar, table, television

Table 39: Classes distribution of CIFAR-100 separated by grouping similar classes together.

Task 1	beaver, dolphin, otter, seal, whale, aquarium fish, flatfish, ray, shark, trout, bee, beetle, butterfly, caterpillar, cockroach, crab, lobster, snail, spider, worm
Task 2	maple, oak, palm, pine, willow, orchids, poppies, roses, sunflowers, tulips, apples, mushrooms, oranges, pears, sweet peppers, cloud, forest, mountain, plain, sea
Task 3	hamster, mouse, rabbit, shrew, squirrel, fox, porcupine, possum, raccoon, skunk, crocodile, dinosaur, lizard, snake, turtle, bear, leopard, lion, tiger, wolf
Task 4	bicycle, bus, motorcycle, pickup truck, train, lawn mower, rocket, streetcar, tank, tractor, bed, chair, couch, table, wardrobe, bridge, castle, house, road, skyscraper
Task 5	baby, boy, girl, man, woman, camel, cattle, chimpanzee, elephant, kangaroo, bottles, bowls, cans, cups, plates, clock, keyboard, lamp, telephone, television

Table 40: Classes distribution of TinyImageNet separated by random seed 3456.

Task 1	Persian cat, clIff, plunger, German shepherd, teddy, American lobster, hourglass, seashore, dumbbell, ice cream, nail, convertible, orangutan, coral reef, go-kart, king penguin, sulphur butterfly, lesser panda, kimono, comic book, cockroach, projectile, lakeside, chimpanzee, bannister, bucket, gondola, koala, lIfeboat, teapot, police van, pill bottle, hog, crane, cash machine, mushroom, water tower, black stork, ice lolly, scorpion
Task 2	sewing machine, lemon, barn, Yorkshire terrier, stopwatch, lawn mower, thatch, pizza, barbershop, organ, computer keyboard, bighorn, cardigan, baboon, snail, syringe, spider web, Labrador retriever, pretzel, pomegranate, tarantula, pop bottle, trilobite, poncho, remote control, European fire salamander, altar, obelisk, binoculars, CD player, ladybug, miniskirt, cannon, wok, potter's wheel, cougar, chest, sunglasses, water jug, picket fence
Task 3	rugby ball, steel arch bridge, refrigerator, espresso, dining table, monarch, brown bear, confectionery, beach wagon, scoreboard, flagpole, potpie, brass, bow tie, brain coral, backpack, chain, bison, pole, beer bottle, grasshopper, tailed frog, lion, torch, abacus, magnetic compass, standard poodle, goose, bullet train, African elephant, gazelle, triumphal arch, iPod, beacon, jinrikisha, fly, dugong, suspension bridge, ox, wooden spoon
Task 4	Egyptian cat, volleyball, rocking chair, bullfrog, apron, swimming trunks, fountain, bikini, school bus, plate, guinea pig, oboe, maypole, goldfish, orange, drumstick, centipede, mashed potato, viaduct, military unIform, banana, sock, bathtub, guacamole, walking stick, pay-phone, alp, lampshade, bell pepper, meat loaf, tabby, tractor, sombrero, gasmask, frying pan, spiny lobster, jellyfish, sandal, vestment, snorkel
Task 5	reel, basketball, parking meter, black widow, umbrella, trolleybus, Arabian camel, space heater, American alligator, albatross, sea cucumber, sea slug, clIff dwelling, boa constrictor, mantis, freight car, Chihuahua, fur coat, beaker, moving van, barrel, acorn, caulIflower, birdhouse, academic gown, golden retriever, neck brace, candle, desk, bee, dam, punching bag, butcher shop, slug, dragonfly, limousine, sports car, turnstile, Christmas stocking, broom

Table 41: Classes distribution of TinyImageNet separated by random seed 5678.

Task 1	reel, lemon, refrigerator, swimming trunks, stopwatch, lawn mower, German shepherd, flagpole, dumbbell, American alligator, backpack, clIff dwelling, sulphur butterfly, kimono, trilobite, sock, bison, projectile, grasshopper, walking stick, lakeside, lion, pay-phone, bullet train, African elephant, birdhouse, gazelle, miniskirt, spiny lobster, pill bottle, hog, cougar, water tower, sunglasses, black stork, suspension bridge, ice lolly, broom, scorpion, picket fence
Task 2	Egyptian cat, bullfrog, basketball, apron, Yorkshire terrier, monarch, pizza, guinea pig, umbrella, barbershop, drumstick, ice cream, nail, space heater, convertible, baboon, snail, orangutan, centipede, syringe, sea slug, mashed potato, military unIform, chain, cockroach, boa constrictor, tailed frog, academic gown, ladybug, golden retriever, cannon, neck brace, iPod, slug, crane, limousine, dugong, water jug, Christmas stocking, wooden spoon
Task 3	sewing machine, clIff, plunger, brown bear, teddy, oboe, maypole, orange, trolleybus, seashore, Arabian camel, brass, bighorn, brain coral, viaduct, king penguin, tarantula, lesser panda, comic book, poncho, mantis, remote control, chimpanzee, alp, lampshade, torch, tabby, lIfeboat, CD player, caulIflower, sombrero, frying pan, dam, beacon, jellyfish, cash machine, mushroom, jinrikisha, chest, ox
Task 4	volleyball, rocking chair, steel arch bridge, espresso, thatch, black widow, school bus, plate, confectionery, beach wagon, American lobster, hourglass, computer keyboard, cardigan, coral reef, albatross, spider web, sea cucumber, beer bottle, bathtub, freight car, altar, beaker, bannister, magnetic compass, moving van, gondola, koala, binoculars, teapot, tractor, triumphal arch, gasmask, desk, bee, punching bag, potter's wheel, butcher shop, vestment, fly
Task 5	rugby ball, Persian cat, barn, parking meter, dining table, fountain, bikini, organ, scoreboard, goldfish, potpie, bow tie, go-kart, Labrador retriever, pretzel, pomegranate, pop bottle, banana, pole, guacamole, Chihuahua, European fire salamander, obelisk, fur coat, bell pepper, bucket, abacus, meat loaf, barrel, standard poodle, goose, acorn, candle, police van, wok, sandal, dragonfly, snorkel, sports car, turnstile

Table 42: Classes distribution of TinyImageNet separated by by grouping similar classes together.

Task 1	school bus, maypole, projectile, freight car, pay-phone, moving van, bullet train, birdhouse, tractor, triumphal arch, cannon, police van, crane, cash machine, jinrikisha, water tower, limousine, sports car, suspension bridge, turnstile, picket fence, refrigerator, barn, lawn mower, barbershop, beach wagon, scoreboard, flagpole, trolleybus, convertible, go-kart, viaduct, pole, bathtub, altar, obelisk, bannister, gondola, lIfeboat, bucket
Task 2	reel, volleyball, rocking chair, basketball, plunger, parking meter, dining table, umbrella, oboe, hourglass, computer keyboard, space heater, backpack, pop bottle, beer bottle, remote control, lampshade, torch, abacus, barrel, CD player, teapot, candle, desk, frying pan, iPod, wok, potter's wheel, pill bottle, snorkel, sunglasses, water jug, broom, wooden spoon, rugby ball, sewing machine, stopwatch, plate, teddy, drumstick
Task 3	Egyptian cat, bullfrog, German shepherd, brown bear, guinea pig, Arabian camel, baboon, Labrador retriever, king penguin, lesser panda, chimpanzee, tabby, goose, koala, gazelle, golden retriever, hog, cougar, black stork, ox, Persian cat, Yorkshire terrier, bighorn, orangutan, American alligator, bison, boa constrictor, Chihuahua, lion, standard poodle, African elephant, cliff, seashore, lakeside, alp, dam, steel arch bridge, fountain, clIff dwelling, magnetic compass
Task 4	monarch, snail, albatross, spider web, sulphur butterfly, tarantula, cockroach, mantis, European fire salamander, ladybug, bee, slug, dragonfly, fly, scorpion, black widow, centipede, grasshopper, tailed frog, goldfish, coral reef, sea cucumber, spiny lobster, jellyfish, American lobster, brain coral, sea slug, trilobite, lemon, banana, guacamole, mushroom, thatch, orange, mashed potato, pomegranate, bell pepper, acorn, cauliflower, binoculars
Task 5	cardigan, sock, fur coat, academic gown, miniskirt, neck brace, sombrero, gasmask, punching bag, sandal, Christmas stocking, apron, swimming trunks, bikini, bow tie, military uniform, kimono, poncho, espresso, pizza, organ, potpie, ice cream, nail, pretzel, beacon, butcher shop, vestment, chest, dugong, ice lolly, confectionery, brass, comic book, meat loaf, dumbbell, syringe, chain, walking stick, beaker